Robotica (2019) volume 37, pp. 161–188. © Cambridge University Press 2018
doi:10.1017/S0263574718000930

Adaptive impedance control of uncertain robot manipulators with saturation effect based on dynamic surface technique and self-recurrent wavelet neural networks

Mohammad Hossein Hamedani, Maryam Zekri* and Farid Sheikholeslam

Department of Electrical and Computer Engineering, Isfahan University of Technology, Isfahan 84156-83111, Iran. E-mails: mh.hamedani@ec.iut.ac.ir, sheikh@cc.iut.ac.ir

(Accepted August 25, 2018. First published online: October 5, 2018)

SUMMARY

Saturation nonlinearities, among the known challenges in control engineering, are ubiquitous in robotic systems and can lead to stability and performance degradation. In this paper, an adaptive dynamic surface impedance (ADSI) control approach is developed for an n-link robotic manipulator by employing self-recurrent wavelet neural networks (SRWNNs) in order to overcome the saturation effect. The proposed control approach is inspired by the theory of dynamic surface control (DSC) and SRWNNs. As a novel application of the dynamic surface method to obtain a simple structure, the target impedance is formulated in the state–space, and effective dynamic surfaces are defined to track the desired impedance behavior. In fact, DSC is used to force the robot manipulator to track the desired impedance, while the robot interacts with an environment. In addition, SRWNNs are applied to approximate the parametric uncertainties and external disturbances in the robot dynamical model. Self-feedback neurons are embedded as memory units in SRWNNs to model the sudden dynamic jumps of the environment. Using Lyapunov's method, an ADSI controller is designed, and adaptation laws are induced to guarantee the stability of the closed-loop system. Finally, simulations are conducted to verify the proper performance of the proposed approach for removing the saturation effect and tracking the target impedance. It is worth noting that the simulation results indicate the robustness of the controller against uncertainties and external disturbances.

KEYWORDS: Adaptive dynamic surface control, Impedance control, Input saturation, Recurrent wavelet neural network

1. Introduction

Over the past decades, increasing attention has been paid to the control design and stability analysis of robot manipulators. Interaction with the environment is one of the essentially important tasks of robot manipulators. By tracking the desired contact force, the manipulator is able to maintain interaction with the environment. However, force control is applicable for manipulation during contact. On the other hand, the manipulator should use a position controller to track the desired path in the workspace. There are many tasks such as welding or painting which robot manipulators should be able to control position and force control objectives together at the same time. Consequently, the position or force controller cannot be easily formulated in order to control a robot manipulator.[1] In ref. [2], in 1985, Hogan formularized impedance control as an implicit force control in which robot manipulators have to track the desired impedance including inertia, damping and stiffness. Because of the nonlinear dynamics of the robot manipulators, control designer requires using nonlinear approaches such as sliding mode control[3] or feedback linearization method[4] to force robot manipulators to track the

* Corresponding author. E-mail: mzekri@cc.iut.ac.ir

https://doi.org/10.1017/S0263574718000930 Published online by Cambridge University Press

desired impedance. Among various methods, feedback linearization is known as a common approach to match impedance of the robot to the desired impedance. Another method is backstepping control[5−8] as a nonlinear approach to control robot manipulator systems. In ref. [5], a support vector regression based command filtered adaptive backstepping method is used to introduce a robust adaptive approach to control a robot system with model uncertainties and disturbances. However, the command filtered backstepping (CFB) is modified and defines the auxiliary states to extend CFB to the case of the robot manipulator. Using neural networks (NNs), Kwan and Lewis[8] proposed the robust backstepping control approach of nonlinear systems to solve two problems of backstepping methods. One of which is that system dynamics should be linear in unknown parameters, and the other one is that analysis of the systems is required to determine regression matrices. Additionally, the backstepping method suffers from a problem called the "explosion of complexity"[9,10] because of repeated differentiation of virtual controllers. To solve this problem, Swaroop *et al.*[9] proposed a dynamic surface control (DSC) technique using a low-pass filter of the synthetic virtual control law at each step of the backstepping procedure. In our work, DSC is used as a nonlinear approach to formulate the target impedance in the state–space and define effective dynamic surfaces error in order to provide a simple structure to track the desired impedance.

In recent decades, many researchers have focused on learning approaches and impedance control in robotic platforms to observe disturbance and uncertainty in the designed controller process.[11−18] There are several learning approaches such as adaptive networks for instance NNs and neuron fuzzy models, which are used to approximate nonlinear functions and unknown system dynamics.[20−25] However, the NNs and fuzzy models cannot be applied to approximate local dynamics. They cannot estimate local time–frequency properties of nonlinear systems such as sudden changes or discontinuity[26] because of their structures. The wavelet transform presents a time–frequency localization of the approximated signal. In wavelet theory, most of the energy of the signal can be well represented by a linear combination of a finite number of wavelet basis functions.[27] Wavelet neural networks (WNNs) have properties such as the high resolution of wavelets, which can be used to estimate local changes,[28−32] learning capability and global approximation of NNs. On the other hand, the WNNs have feed-forward structures such as NNs, which are able to present a static model. However, they are unable to represent a dynamic mapping. To avoid these problems, in ref. [19], the self-recurrent WNN (SRWNN), which has the properties of recurrent neural networks[33,34] and local approximation of WNNs, has been proposed to control a flexible-joint robot. However, in ref. [19], the dynamic surface approach is not formulated for impedance controller. Therefore, SRWNNs can be used to control and estimate nonlinear dynamic systems.[35,36] SRWNNs have a mother-wavelet layer composed of self-feedback neurons. Actually, they can store the past information of the network to model sudden jumps of the environment. Since robot manipulators usually work in uncertain environments, nonlinearity features such as uncertainties and disturbances commonly happen. Because of the above-mentioned reasons, in our study, SRWNNs are chosen to model the uncertainty of the model dynamic of the robot and disturbances.

One of the known challenges in robotic systems control is how to deal with actuator saturation, which increases the cost of the control design such as an overshoot or a large tracking error.[1] Additionally, input saturation can damage the actuators and the system. Additionally, large disturbances and uncertainties can be considered one of the sources of the actuator saturation. This problem can occur when the uncertainties and disturbances are very large in the systems so that the actuators cannot compensate them using their own signal constraints. Therefore, removing uncertainties and disturbances is the essentially important task of a controller to prevent actuator saturation. To solve the problem, many researchers have developed various methods to handle the control design related to saturation. Santibañez *et al.*[37] supposed that the parameters of dynamic systems and saturator structure are available and presented the nonlinear Proportional-Integral-Derivative (PID) controller for robotic manipulators. In ref. [1], using Radial Basis Function Networks (RBFNs) in the presence of input saturation, an adaptive neural impedance control of a robotic manipulator has been presented. They used an auxiliary system to control input saturation leading to the complexity of the problem. Huang *et al.*[38] proposed a solution to the global tracking and stabilization control of a robot in the presence of input saturation. In addition, in ref. [39], an adaptive control has been designed to remove the external disturbance, saturation and dead-zone of nonlinear systems.

https://doi.org/10.1017/S0263574718000930 Published online by Cambridge University Press

In this paper, we present a robust impedance control of robot manipulators with model uncertainties via adaptive DSC technique using SRWNN to solve input saturation. As a novel application of the dynamic surface method to obtain a simple structure, the target impedance is formulated in the state–space. Consequently, the effective dynamic surfaces are defined to track the desired impedance behavior. Proposed controller compensates distributing forces by modeling environment and parametric uncertainties without any knowledge of the actual dynamical model. To force the robot manipulator to track the desired impedance, an effective dynamic surface based on Lyapunov function is designed. In the proposed control system, DCS is used to eliminate the drawback of the "explosion of complexity" in the backstepping approach caused by repeated differentiation of virtual controllers. To avoid input saturation, the SRWNNs with self-feedback neurons as memory units are used to observe unknown dynamic model uncertainty terms of robotic systems and external disturbances. The adaptation laws for all the parameters of SRWNN induced from Lyapunov stability analysis are used to guarantee the uniformly ultimately bounded signals in the closed-loop system. In addition, various simulation cases are conducted to compare the performance of the proposed controller with other methods.

The rest of this paper is organized as follows. In Section 2, the preliminaries and system dynamics of robot manipulators are presented. In Section 3, using SRWNN for the tracking desired impedance of robot manipulators, the adaptive DSC system is proposed to solve the robust control problem. Additionally, the performance of the proposed control systems is analyzed by the Lyapunov stability theory. Section 4 shows the performance of the proposed method by simulations, and Section 5 concludes with a short summary of the paper.

2. Preliminaries and Problem Formulation

The general nominal dynamic of an n-link robot manipulator can be described using the following forms:[3]

$$M(q)\ddot{q} + C(q,\dot{q})\dot{q} + G(q) + J^T(q)F + \tilde{f}(t) = \tau \tag{1}$$

where $q \in \mathbb{R}^{n\times 1}$ is joint displacement vector, $\tau \in \mathbb{R}^{n\times 1}$ is the applied joint torque, $M(q) \in \mathbb{R}^{n\times n}$ is the inertia matrix, $C(q,\dot{q})\dot{q} \in \mathbb{R}^{n\times 1}$ is the Coriolis and centrifugal vector, $G(q) \in \mathbb{R}^{n\times 1}$ is the gravitational vector, F is the interaction forces vector and $\tilde{f}(t)$, as the external disturbances, introduces the uncertainty of the interaction forces. Assuming that the system states q, $\dot{q}$ and interaction force F are available for feedback. $J(q)$ is the Jacobin matrix such that

$$J(q) = \frac{\partial x(q)}{\partial q} \tag{2}$$

where x vector includes the position and orientation of the end-effector. Moreover, $J(q)$ is assumed a nonsingular matrix.

Property 1 [3]. For any finite workspace Ω, $M(q)$ is a symmetric positive definite matrix. Moreover, there exist $k' > 0$ and $k'' > 0$ such that

$$k'I \le M(q) \le k''I \quad \forall q \in \Omega \tag{3}$$

Property 2 [40]. The matrix $N(q,\dot{q}) = \dot{M}(q) - 2C(q,\dot{q})$ is a skew-symmetric matrix.

Assume that the nominal values of $M(q), C(q,\dot{q})$ and $G(q)$ may be different from the actual values $\hat{M}(q)$, $\hat{C}(q,\dot{q})$ and $\hat{G}(q)$, respectively, due to model uncertainty and external disturbance.

Assumption 1. Suppose that, for a given manipulator robot, only the nominal values $M(q), C(q,\dot{q})$ and $G(q)$ are known, but the actual values $\hat{M}(q)$, $\hat{C}(q,\dot{q})$ and $\hat{G}(q)$ including model uncertainties and external disturbance $\tilde{f}(t)$ are unknown.

https://doi.org/10.1017/S0263574718000930 Published online by Cambridge University Press

Assumption 2 [3]. Modeling errors are not available. However, they are bounded as follows:

$$\begin{array}{ll} |\Delta M(q)| \le \delta M(q) & \Delta M(q) = M(q) - \hat{M}(q) \\ |\Delta C(q,\dot{q})| \le \delta C(q,\dot{q}) & \Delta C(q,\dot{q}) = C(q,\dot{q}) - \hat{C}(q,\dot{q}) \\ |\Delta G(q)| \le \delta G(q) & \Delta G(q) = G(q) - \hat{G}(q) \\ \left|\tilde{f}(t)\right| \le \delta \tilde{f}(t) & \end{array} \tag{4}$$

The dynamic of n-link rigid robotic system in Cartesian space is described by

$$M(x)\ddot{x} + C(x,\dot{x})\dot{x} + G(x) + F + \tilde{F}(x,t) = T \tag{5}$$

where

$$\begin{array}{l} M(x) = J^{-T}(q) M(q) J^{-1}(q) \\ C(x,\dot{x}) = J^{-T}(q) C(q,\dot{q}) J^{-1}(q) - J^{-T}(q) M(q) J^{-1}(q) \dot{J}(q) J^{-1}(q) \\ G(x) = J^{-T}(q) G(q) \\ \tilde{F}(x,t) = J^{-T}(q) \tilde{f}(t) \\ T = J^{-T}(q)\tau \end{array} \tag{6}$$

The actual n-link robot dynamic (5) can be expressed in Cartesian space using (6):

$$\hat{M}(x)\ddot{x} + \hat{C}(x,\dot{x})\dot{x} + \hat{G}(x) + F + \tilde{F}(x,t) = T \tag{7}$$

The actual robot dynamics (7) can be rewritten in the following formulation using the nominal model:

$$M(x)\ddot{x} + C(x,\dot{x})\dot{x} + G(x) + F + \Pi = T \tag{8}$$

where Π is defined as (9) to denote the uncertainty of robot dynamics:

$$\begin{aligned} \Pi(x,\ \dot{x}, F, T) = -M(x)\hat{M}(x)^{-1} \times \left\{-\tilde{F}(x,t) - \hat{C}(x,\dot{x})\dot{x} - \hat{G}(x) - F + T\right\} \\ + \{-C(x,\dot{x})\dot{x} - G(x) - F + T\} \end{aligned} \tag{9}$$

By considering the state–space variable as $x_1 = x,\ x_2 = \dot{x}$, the robot dynamic system with uncertainty terms (8) can be described as follows:

$$\dot{x}_1 = x_2 \tag{10}$$

$$\dot{x}_2 = M^{-1}(x_1)[-C(x_1,x_2)x_2 - G(x_1) + T - F] + \mathrm{H}(x_1,x_2,F,T) \tag{11}$$

where

$$\mathrm{H}(x_1,x_2,F,T) = -M^{-1}(x_1)\ \Pi(x_1,x_2,F,T) \tag{12}$$

In fact, the control input T and the interaction force F are only the functions of $x_1,\ x_2, X_d$ in which $X_d = [x_d\ \dot{x}_d\ \ddot{x}_d]$ denotes desired position, velocity and acceleration, respectively, in Cartesian space. Hence, (11) can be expressed as

$$\dot{x}_2 = M^{-1}(x_1)[-C(x_1,x_2)x_2 - G(x_1) + T - F] + \mathrm{H}(x_1,x_2,X_d) \tag{13}$$

$$\mathrm{H}(x_1,x_2,X_d) = -M^{-1}(x_1)\ \Pi(x_1,x_2,X_d) \tag{14}$$

According to (10) and (13), $\mathrm{H}(x_1,x_2,X_d)$ presents unknown dynamic uncertainty and SRWNN is formulated to estimate (14). In the following, the adaptive dynamic surface impedance (ADSI) control is proposed.

https://doi.org/10.1017/S0263574718000930 Published online by Cambridge University Press

3. Proposed Controller

Assume that we have the robot manipulator models (10) and (13) with uncertainty term (14). The desired controller should determine the term $\mathrm{H}(x_1, x_2, X_d)$ accurately in order to remove it as much as possible. Additionally, the controller should be able to force the robot impedance to follow the defined target impedance. To realize that, the target impedance is formulated in state–space and the objective controls are introduced in Section 3.1. Then, the SRWNN is applied to observe uncertainties and disturbances in Section 3.2. Finally, in Section 3.3, Theorems 1 and 2 are presented to design the proposed control impedance approach for robot manipulators using dynamic surface; an adaptive law is, then, introduced to update the network parameters.

3.1. Objective control

The desired impedance is specified as follows:[3]

$$\begin{aligned} M_m\ddot{e} + B_m\dot{e} + K_m e &= -F(t) \\ e(t) &= x(t) - x_{vd}(t) \end{aligned} \tag{15}$$

where M_m, B_m and $K_m \in \mathbb{R}^{m\times m}$, $m \leq 6$ are the desired inertia, damping and stiffness, respectively, $x_{vd}(t) \in \mathbb{R}^m$ is the virtual desired motion trajectory in the world space, which is bounded, smooth and twice differentiable. Frequently, M_m, B_m and K_m are selected as a diagonal matrix to obtain a decoupled response. According to (15), while the robot moves in free space, $x_{vd} = x \quad \forall t > 0$, $F(t) = 0$, and when the robot interacts with the environment, the end-effector response is to comply with the contact forces defined by target impedance.

The objective of the ADSI control is to design a control approach so that the impedance of the robot manipulator tracks the given target impedance (15) under assuming uncertainties and disturbances modeling (14). To that end, we define $z_1 = x$, $z_2 = \dot{x}$; the desired impedance terms (15) can be described as follows:

$$\dot{z}_1 = z_2 \tag{16}$$

$$\dot{z}_2 = \ddot{x}_{vd} - M_m^{-1}\left[F(t) + B_m(z_2 - \dot{x}_{vd}) + K_m(z_1 - x_{vd})\right] \tag{17}$$

To realize acceptable tracking of the desired impedance (15), the dynamics of (10) and (13) should track Eqs. (16) and (17). Our next task, in this constructive route, is to use SRWNN as an uncertainty observer in order to avoid input saturation and the state vector x_1, x_2 track desired state vector represented by z_1, z_2. Then, an adaptive law is developed to adjust all parameters of SRWNN so that all uniformly ultimately bounded signals in the closed-loop system are guaranteed.

3.2. SRWNN structure

Since robot manipulators operate in different workspaces, the properties of the environment such as stiffness or damping are variously unknown. Thus, offline learning methods are not served, and online learning approaches with fast convergence should necessarily be applied. Hence, SRWNN is considered as an adaptive network to observe dynamic uncertainties and disturbances.

In this study, the structure of the SRWNN model is shown in Fig. 1. The network consists of four layers, i.e., input layer, wavelet layer, product layer and the output layer. Each node of the wavelet layer consists of a mother wavelet and a self-feedback loop as a memory unit to store information in the second layer. Input and output vectors of SRWNN are defined as $x_q = [q_1 \ldots q_n\ q_{(n+1)r} \ldots q_{2nr}] = [x_{q1} \quad \ldots \quad x_{qN_i}]$ and y, respectively. $q_1 \ldots q_n$ are the joint displacements of the robot manipulator and $q_{(n+1)r} \ldots q_{2nr}$ are the joint displacements references. N_i is the number of inputs of the network, and N_w is the number of output weights. The first derivative of Gaussian function, i.e., $\Phi(x) = (-x)e^{-\frac{1}{2}x^2}$, is used as a mother wavelet. Inputs u_{ji} of the wavelet nodes can be defined as follows:

$$u_{ji} = x_{q_i} + \Phi_{ji} z^{-1} \cdot \theta_{ji} \tag{18}$$

https://doi.org/10.1017/S0263574718000930 Published online by Cambridge University Press

where θ_{ji} represents the information storage parameters and z^{-1} denotes time delay. The main aspect of SRWWN is the term z^{-1}, which stores the past information and current dynamics of the network for the next sample.

The outputs of product layer are given by

$$\Psi_j = \prod_{i=1}^{N_i} \Phi\left(z_{ji}\right) \quad \text{with} \quad z_{ji} = \frac{u_{ji} - a_{ji}}{d_{ji}}, \quad j = 1, \ldots, N_w \tag{19}$$

where a_{ji} and d_{ji} are the translation and the dilation factors of the mother wavelet, respectively.

The output of SRWNN can be denoted as follows:

$$y = \sum_{j=1}^{N_w} w_j \Psi_j + \sum_{i=1}^{Ni} b_i x_{qi} \tag{20}$$

where w_j is the weights between product nodes and output nodes; b_i is the weight between input nodes and output nodes. The first term in the right-hand side of (20) reveals that SRWNN is a kind of NN that uses wavelet functions as the activation function. For this reason, SRWNN can estimate discontinuities or sudden changes of nonlinear functions.

As mentioned about the online learning approach, the parameters of SRWNN, i.e., b_i, a_{ji}, d_{ji}, θ_{ji} and w_j $j = 1, \ldots, N_w$ need to be trained by adaptation laws in the sense of Lyapunov stability analysis. The parameter vector W is defined as follows:

$$\begin{aligned} W = [&b_1\ b_2 \ldots b_{N_i}\ a_{11}\ a_{12} \ldots a_{1N_i}\ a_{21} \ldots a_{2N_i} \ldots a_{N_wN_i} \\ &d_{11}\ d_{12} \ldots d_{1N_i}\ d_{21} \ldots d_{2N_i} \ldots d_{N_wN_i}\ \theta_{11}\ \theta_{12} \ldots \theta_{1N_i}\ \theta_{21} \ldots \theta_{2N_i} \ldots \theta_{N_wN_i}\ w_1 \ldots w_{N_w}] \end{aligned} \tag{21}$$

Remark 1. Using the inverse kinematics, the authors obtained the generalized coordinates of robot manipulators $q = [q_1 \ldots q_n]^{\mathrm{T}}$ from $x = [x_1 \ldots x_m]^{\mathrm{T}}$, where $x \in \mathbb{R}^{m\times 1}$, $m \leq 6$ are the Cartesian coordinates of end-effector in the world space. In this paper, generalized coordinates q and q_r, available by reading sensors and inverse kinematics of the target impedance models (16) and (17), respectively, are used as the inputs of SRWNN. The structure of the SRWNN for a two-link robot manipulator is shown in Fig. 1.

3.3. Adaptive dynamic surface impedance control

In this subsection, an adaptive controller and adaptive law are obtained. Since the study of the SRWNN is used to estimate the uncertainties and disturbances, formulation of the estimator is emphasized.

Assumption 3 [19]. Assume that input X of the SRWNN belongs to a compact set K_X. To approximate the nonlinear function $Y(X)$, SRWNN is used. The optimal parameter vector W^* of the SRWNN is given as follows:

$$W^* = \arg\min_{\hat{W}\in\mathcal{K}_w} \left[\sup_{X\in\mathcal{K}_X} \left\| Y(X) - \hat{Y}\left(X|\hat{W}\right)\right\|\right] \tag{22}$$

where $\mathcal{K}_W$ is a compact set of the parameter vector and $\mathcal{K}_W = \{\hat{W} |\ \|\hat{W}\| \leq \mathcal{R}_w\}$ denotes a ball of radius $\mathcal{R}_w$; it is assumed that the optimal parameter W^* is also restricted to $\mathcal{K}_W$. $\hat{W}$ is the estimated vectors of the parameters vector (21), and $\hat{Y}$ is the estimation of the output network.

The uncertainty equation (14) can be estimated by the SRWNN as follows:

$$\begin{aligned} \mathrm{H}(X) &= \mathrm{H}^*(X|W^*) + \varepsilon \\ &= \hat{\mathrm{H}}\left(X|\hat{W}\right) + \left[\mathrm{H}^*(X|W^*) - \hat{\mathrm{H}}\left(X|\hat{W}\right)\right] + \varepsilon \end{aligned} \tag{23}$$

where ε is the estimation error, $X = (x_1, x_2, X_d)$ and $\hat{W} = \mathrm{diag}\,[\hat{W}_i]$ is the estimated parameters matrix for $i = 1, 2, \ldots, l$, where l denotes dimensions of H.

https://doi.org/10.1017/S0263574718000930 Published online by Cambridge University Press

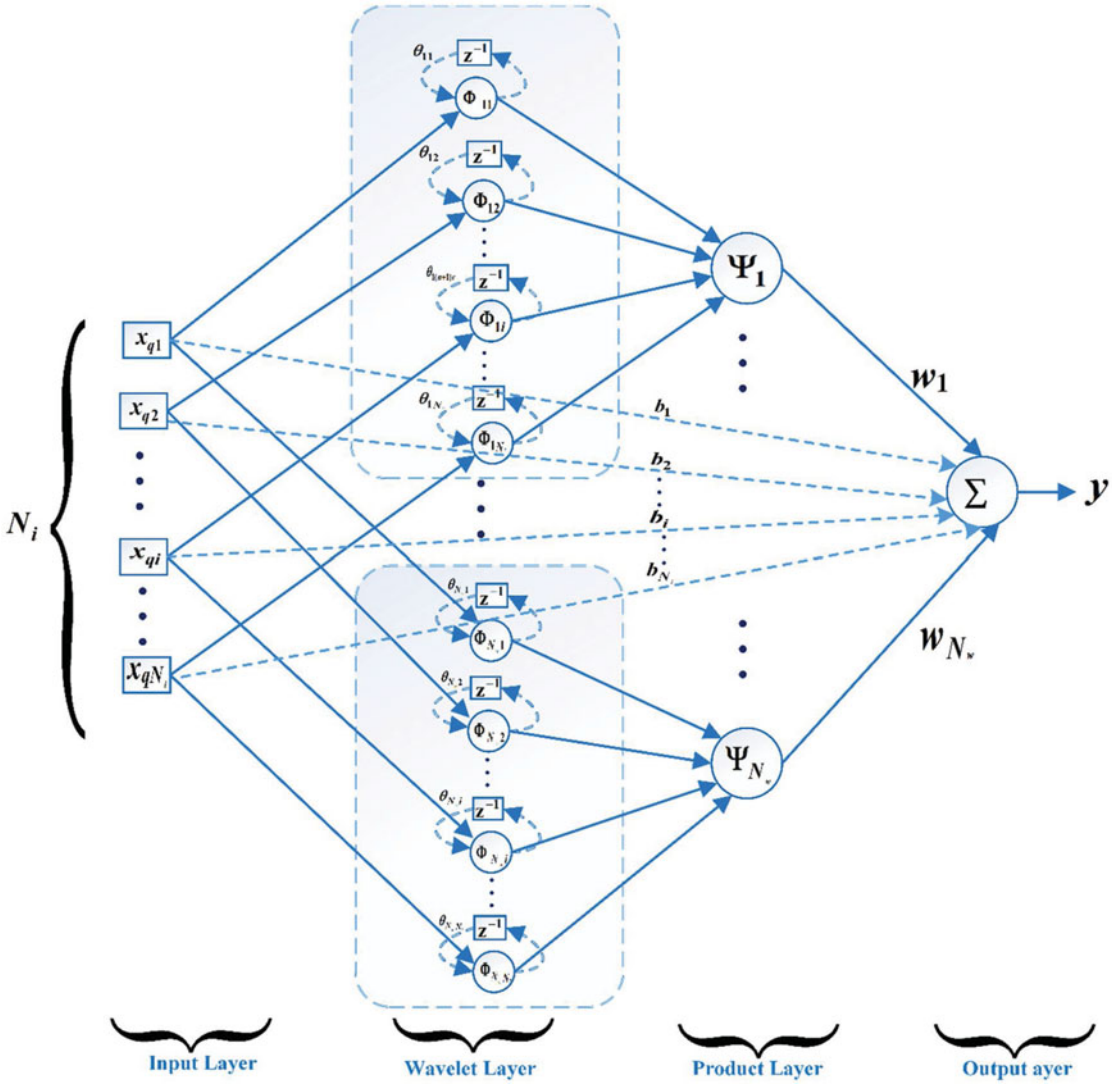


Fig. 1. SRWNN structure of robot manipulator.

Assumption 4. Assume that the optimal weight matrix is bounded as follows:

$$\left\|W^*\right\|_F \leq W_M \tag{24}$$

where $\|\ .\|_F$ denotes the Frobenius norm.

According to Taylor series expansion of $\mathrm{H}^*(X|W^*)$ around $\hat{W}$, we have the following:

$$\mathrm{H}^*\left(X|W^*\right) = \hat{\mathrm{H}}\left(X|\hat{W}\right) + \tilde{W}^T\Theta_W + O\left(W^*, \hat{W}\right) \tag{25}$$

where $O(W^*, \hat{W})$ are high-order terms and

$$\tilde{W} = W^* - \hat{W} \tag{26}$$

$$\Theta_W = \left[\frac{\partial \hat{H}_1}{\partial \hat{W}_1},\ \frac{\partial \hat{H}_2}{\partial \hat{W}_2},\ \ldots,\ \frac{\partial \hat{H}_l}{\partial \hat{W}_l}\right]^{\mathrm{T}} \tag{27}$$

https://doi.org/10.1017/S0263574718000930 Published online by Cambridge University Press

Substituting (25) into (23), we have the following:

$$\begin{aligned} \mathrm{H}(X) &= \mathrm{H}^*(X|W^*) + \varepsilon \\ &= \hat{\mathrm{H}}\left(X|\hat{W}\right) + \tilde{W}^T \Theta_W + \eta \end{aligned} \tag{28}$$

$$\|\eta\| \leq \rho \quad \rho > 0 \tag{29}$$

where $\eta = O(W^*, \hat{W}) + \varepsilon$.

Accordingly, the ADSI controller is designed as follows.

In the first step, the virtual control law is designed for x_2. To reach this aim, the first error surface is defined as follows:

$$S_1 = x_1 - z_1 \tag{30}$$

and its derivative is

$$\dot{S}_1 = x_2 - z_2 \tag{31}$$

A virtual control $\bar{x}_2$ is designed to drive $S_1 \to 0$ as follows:

$$\bar{x}_2 = -K_1 S_1 + z_2 K_1 > 0 \tag{32}$$

Because of multiple surface sliding control drawbacks[10], $\bar{x}_2$ is passed through a first-order filter with the time constant $\tau_2 > 0$ as

$$\tau_2 \dot{x}_{2f} + x_{2f} = \bar{x}_2 \quad x_{2f}(0) = \bar{x}_2(0) \tag{33}$$

In the second step, the actual control law for T is designed. Therefore, the second error surface S_2, with filtering virtual control vector x_{2f}, is defined as follows:

$$S_2 = x_2 - x_{2f} \tag{34}$$

and its derivative is

$$\dot{S}_2 = \dot{x}_2 - \dot{x}_{2f} \tag{35}$$

Substituting (13) and (33) in (35) yields

$$\dot{S}_2 = M^{-1}(x_1)\left[-C(x_1, x_2)x_2 - G(x_1) + T - F\right] + \mathrm{H}(x) - \frac{\bar{x}_2 - x_{2f}}{\tau_2} \tag{36}$$

We now propose a signal control T such that $S_2 \to 0$. As mentioned in Section 3.1, the control objective is to design an ADSI control using SRWNN as an uncertainty observer for the state vector $x_1, \ x_2$ to track desired state vector represented by $z_1, \ z_2$. Accordingly, the following structure control in Fig. 2 is proposed, and the adaptive law is presented in Theorem 1. Finally, error vector boundedness is proved by Theorem 2 using the proposed control approach.

Figure 2 shows the block diagram of the proposed ADSI controller for a two-link robot manipulator. In this figure, the generated target impedance block is responsible for determining the desired state vector z_1, z_2 as position and velocity of the reference trajectory. SRWNN block, based on the inputs, estimates H in Eq. (14) as uncertainty and disturbance terms. The virtual control and the first-order filter generate $\bar{x}_2$ and x_{2f}, respectively. Finally, the actual controller block prepares the control signal using Eq. (37) for the actuators of the robot manipulator.

Theorem 1. Consider the closed-loop system (Fig. 2) and the robot manipulator (1), the system achieves the desired impedance if the following control torque is applied:

$$\tau = J^T\left[F + G(x) + C(x, \dot{x})\dot{x} + M(x)\left(-K_2 S_2 - \hat{\mathrm{H}}(x) + \frac{\bar{x}_2 - x_{2f}}{\tau_2}\right)\right] \tag{37}$$

https://doi.org/10.1017/S0263574718000930 Published online by Cambridge University Press

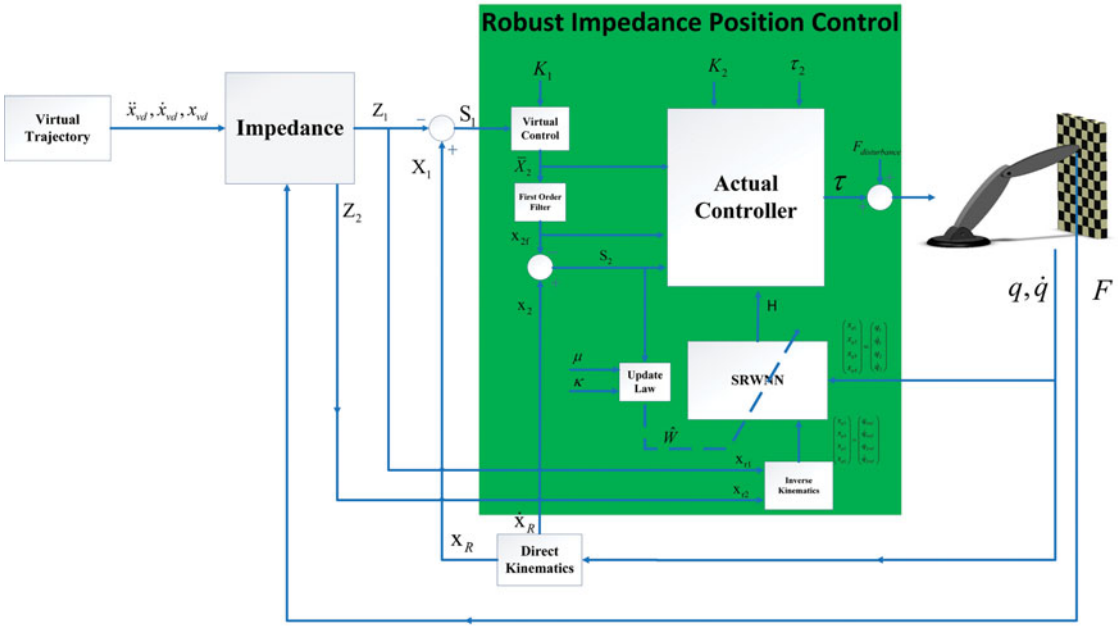


Fig. 2. Block diagram of the proposed ADSI controller for two-link robot manipulator.

If Assumptions 2–4 are satisfied, then the adaptation law for updating SRWNN parameters is designed as follows:

$$\dot{\hat{W}}_i = \mu_i \Theta_{w,i} S_{2,i} - \kappa \mu_i \hat{W}_i \quad i = 1, 2, \ldots, l \tag{38}$$

where κ, K_2 and μ_i are the positive definite; $\Theta_{w,i}$ and $S_{2,i}$ are the ith elements of Θ_W and S_2, respectively. Then, the closed-loop control system is uniformly ultimately bounded.

Proof. Analytic expression of the closed-loop system is driven via surface errors (S_1 and S_2) and boundary layer error y_2. Substituting (34) in (31) yields

$$\dot{S}_1 = S_2 + x_{2f} - z_2 \tag{39}$$

□

Boundary layer error is defined as follows:

$$\begin{aligned} y_2 &= x_{2f} - \bar{x}_2 \\ &= x_{2f} + K_1 S_1 - z_2 \end{aligned} \tag{40}$$

and its derivative is

$$\begin{aligned} \dot{y}_2 &= \dot{x}_{2f} + K_1 \dot{S}_1 - \dot{z}_2 \\ &= \tfrac{\bar{x}_2 - x_{2f}}{\tau_2} + K_1 \dot{S}_1 - \dot{z}_2 \end{aligned} \tag{41}$$

Substituting (39) and (40) in (41) yields

$$\begin{aligned} \dot{y}_2 &= \tfrac{\bar{x}_2 - x_{2f}}{\tau_2} + K_1 S_2 + K_1 x_{2f} - \dot{z}_2 \\ &= -\tfrac{y_2}{\tau_2} + R_2\left(S_2, x_{2f}, X_d\right) \end{aligned} \tag{42}$$

where $R_2(S_2, x_{2f}, X_d) = K_1 S_2 + K_1 x_{2f} - \dot{z}_2$. From Eqs. (38), (39) and (40), the dynamic surfaces can be rewritten as follows:

$$\begin{aligned} \dot{S}_1 &= S_2 + y_2 - K_1 S_1 \\ \dot{S}_2 &= -K_2 S_2 + \tilde{W}^T \Theta_W + \eta \end{aligned} \tag{43}$$

https://doi.org/10.1017/S0263574718000930 Published online by Cambridge University Press

Now, Lyapunov function is chosen as follows:

$$V = \frac{1}{2}\left[S_1^T S_1 + S_2^T S_2 + y_2^T y_2 + tr\left(\tilde{W}^T \mu^{-1} \tilde{W}\right)\right] \tag{44}$$

where μ is a positive definite diagonal matrix.

Differentiating (44) with respect to time and substituting (42) and (43) yield

$$\begin{aligned}
\dot{V} &= S_1^T \dot{S}_1 + S_2^T \dot{S}_2 + y_2^T \dot{y}_2 - tr\left(\tilde{W}^T \mu^{-1} \dot{\hat{W}}\right) \\
&= S_1^T \left(S_2 + y_2 - K_1 S_1\right) + S_2^T \left(-K_2 S_2 + \tilde{W}^T \Theta_W + \eta\right) + y_2^T \left(-\frac{y_2}{\tau_2} + R_2\right) - tr\left(\tilde{W}^T \mu^{-1} \dot{\hat{W}}\right) \\
&= S_1^T \left(S_2 + y_2 - K_1 S_1\right) + S_2^T \left(-K_2 S_2 + \eta\right) + y_2^T \left(-\frac{y_2}{\tau_2} + R_2\right) - \sum\nolimits_{i=1}^{l} \tilde{W}_i^T \left(\Theta_W S_{2,i} - \mu^{-1} \dot{\hat{W}}\right)
\end{aligned} \tag{45}$$

Then, substituting (38) into (45) yields

$$\dot{V} \leq \|S_1\| \|S_2\| + \|S_1\| \|y_2\| - K_1 \|S_1\|^2 - K_2 \|S_2\| + \|S_2\| \eta - \frac{\|y_2\|^2}{\tau_2} + \left|y_2^T R_2\right| + \kappa tr\left(\tilde{W}^T \hat{W}\right) \tag{46}$$

For any finite workspace, Ω, similar Property 1 and boundedness of X_d, there exists a positive constant P_2 such that $\|R_2\| \leq P_2$. Using Assumption 4, Eq. (26) and the fact that $2z_1 z_2 \leq z_1^2 + z_2^2$

$$\begin{aligned}
\dot{V} \leq\ & \|S_1\|^2 + \frac{1}{4}\|S_2\|^2 + \|S_1\|^2 + \frac{1}{4}\|y_2\|^2 - K_1 \|S_1\|^2 - K_2 \|S_2\| + \|S_2\|^2 - \frac{\|y_2\|^2}{\tau_2} + \|y_2\|^2 \\
& + \frac{1}{4}\left(P_2^2\right) + \frac{1}{4}\left(\rho^2\right) + \kappa\left(\left\|\tilde{W}\right\|_F W_M - \left\|\tilde{W}\right\|_F^2\right)
\end{aligned} \tag{47}$$

Such that $\dot{V} \leq 0$, we choose $K_1 = 2 + K_1^*$, $K_2 = \frac{5}{4} + K_2^*$ and $\frac{1}{\tau_2} = \frac{5}{4} + \lambda_2$, and substitution into (47) yields

$$\begin{aligned}
\dot{V} \leq\ & -K_1^* \|S_1\|^2 - K_2^* \|S_1\|^2 - \lambda_2 \|y_2\|^2 - \frac{1}{2}\kappa \left\|\tilde{W}\right\|_F^2 - \frac{1}{2}\kappa\left(\left\|\tilde{W}\right\|_F - W_M\right)^2 \\
& + \frac{1}{2}\kappa W_M^2 + \frac{1}{4}\rho^2 + \frac{1}{4}P_2^2 \\
\leq\ & -K_1^* \|S_1\|^2 - K_2^* \|S_1\|^2 - \lambda_2 \|y_2\|^2 - \frac{1}{2}\kappa \left\|\tilde{W}\right\|_F^2 + O
\end{aligned} \tag{48}$$

where $K_1^*(t) > \bar{K}_1^* > 0$, $K_2^*(t) > \bar{K}_2^* > 0$; statement O is the high-order term which introduces the uncertainty presence.

Let us choose constant ζ satisfying condition as follows:

$$0 < \zeta < \min\left[\bar{K}_1^*,\ \bar{K}_2^*,\ \lambda_2,\ \frac{\kappa \mu_m}{2}\right] \tag{49}$$

where μ_m is the minimum eigenvalue of μ. Hence, we obtain the following:

$$\dot{V} \leq -2\zeta V + O \tag{50}$$

Equation (50) implies that $\dot{V} < 0$ when $V > \mathrm{O}/2\zeta$. The surface errors (S_1 and S_2), the boundary layer error y_2 and the weight estimation error $\tilde{W}$ are all uniformly ultimately bounded in the following

https://doi.org/10.1017/S0263574718000930 Published online by Cambridge University Press

compact set $\mathcal{F}$:

$$\mathcal{F} = \left\{ S_1,\ S_2, y_2, \tilde{W} \mid \|S_1\|^2 + \|S_2\|^2 + \|y_2\|^2 + \frac{1}{\mu_m} \times \left\|\tilde{W}\right\|_F^2) \leq \frac{\mathrm{O}}{\zeta} \right\} \tag{51}$$

Compact set $\mathcal{F}$ can be kept arbitrarily small choosing $\bar{K}_1^*,\ \bar{K}_2^*,\ \lambda_2, \mu$ and κ. The proof of Theorem 1 is thus established.

Now, Theorem 2 is presented to verify that the error vector bounds for proposed control system are bounded.

Theorem 2. Error vector including surface errors, boundary layer errors and estimation errors is defined as follows:

$$Z = \left[S_1^T\ S_2^T\ y_2^T\ \left\|\tilde{W}\right\|_F \right]^{\mathrm{T}} \tag{52}$$

which converges asymptotically to the compact set

$$\Omega_z := \{ Z \in \mathbb{R}^{l_z \times 1} \mid \left\| Z \leq \sqrt{M} \right\| \} \tag{53}$$

where $M = 2(V(0)e^{-2\zeta t} + \frac{O}{2\zeta})$ with ζ and O given in (49) and (50).

Proof. Multiplying (50) by $e^{2\zeta t}$ yields

$$\frac{\mathrm{d}}{\mathrm{d}t}\left(V e^{2\zeta t}\right) \leq O e^{2\zeta t}. \tag{54}$$

□

Integrating (54), we have the following:

$$V(t) \leq V(0)\, e^{-2\zeta t} - \frac{O}{2\zeta} e^{-2\zeta t} + \frac{O}{2\zeta} \leq V(0) + \frac{O}{2\zeta} \tag{55}$$

For Z, we have the following:

$$\frac{1}{2} Z^T Z \leq V(0)\, e^{-2\zeta t} + \frac{O}{2\zeta} \tag{56}$$

Now, we can obtain

$$\|Z\| \leq \sqrt{M} \tag{57}$$

where $M = 2(V(0)e^{-2\zeta t} + \frac{O}{2\zeta})$, and the compact set introduced in (51) is proved.

Remark 2. In conclusion, if the disturbance and uncertainty effects (14) do not exist in systems, the adaptation law (38) is not necessary, and hence, the high-order term $O = 0$ in (50). Consequently, the closed-loop system is asymptotically stable according to (56).

4. Simulation Study

To verify the effectiveness and robustness of the proposed ADSI controller (37) for two-link robot manipulator, simulations are performed with input saturation and large disturbance. Consider the 2-DOF robotic manipulator with two revolution joints in the vertical plane, as shown in Fig. 3. Let m_i and l_i be the mass and length of the link i, respectively, lc_i be the distance from joint $i - 1$ to the center of the mass of the link i and I_i be the moment of inertia of the link i about an axis coming out of the page passing through the center of mass of link i, $i = 1, 2$.

https://doi.org/10.1017/S0263574718000930 Published online by Cambridge University Press

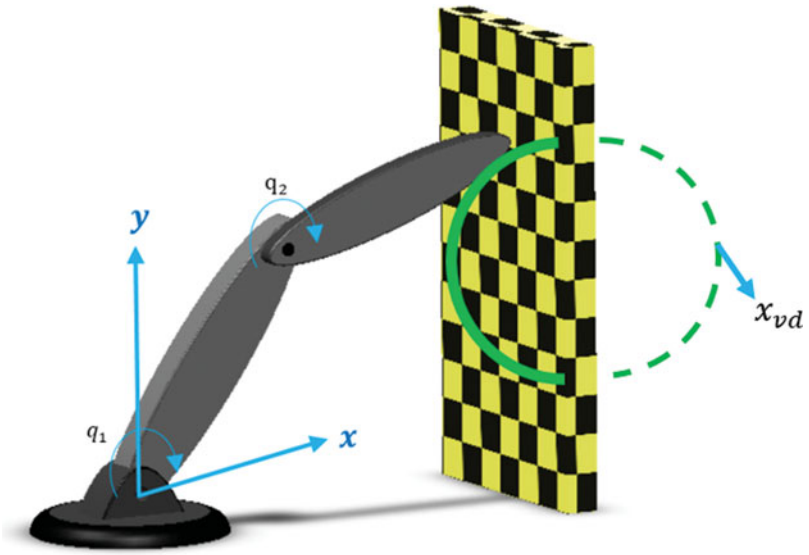


Fig. 3. Two-link robot manipulator.

We define the generalized coordinates to describe the dynamic equation of robot (1) as follows:

$$q = \begin{bmatrix} q_1 \\ q_2 \end{bmatrix} = \begin{bmatrix} \theta_1 \\ \theta_2 \end{bmatrix} \tag{58}$$

Then, the dynamics of the robot can be expressed as (1), where

$$\begin{aligned} G(q) &= \begin{bmatrix} G_{11} \\ G_{21} \end{bmatrix} \\ M(q) &= \begin{bmatrix} M_{11} & M_{12} \\ M_{21} & M_{22} \end{bmatrix} \\ C(q, \dot{q}) &= \begin{bmatrix} C_{11} & C_{12} \\ C_{21} & C_{22} \end{bmatrix} \end{aligned} \tag{59}$$

and

$$\begin{aligned} G_{11} &= (m_1 l_{c2} + m_2 l_1)\, g \cos(q_1) + m_2 l_{c2} g \cos(q_1 + q_2) \\ G_{21} &= m_2 l_{c2} g \cos(q_1 + q_2) \\ M_{11} &= m_1 l_{c1}^2 + m_2 \left(l_1^2 + l_{c2}^2 + 2 l_1 l_{c2} \cos(q_2)\right) + I_1 + I_2 \\ M_{12} &= m_2 \left(l_{c2}^2 + l_1 l_{c2} \cos(q_2)\right) + I_2 \\ M_{21} &= m_2 \left(l_{c2}^2 + l_1 l_{c2} \cos(q_2)\right) + I_2 \\ M_{22} &= m_2 l_{c2}^2 + I_2 \\ C_{11} &= -m_2 l_{c2} \dot{q}_2 \sin(q_2) \\ C_{12} &= -m_2 l_1 l_{c2} (\dot{q}_1 + \dot{q}_2) \sin(q_2) \\ C_{21} &= m_2 l_1 l_{c2} \dot{q}_1 \sin(q_2) \\ C_{22} &= 0 \end{aligned} \tag{60}$$

The Jacobian matrix is written as follows:

$$J(q) = \begin{bmatrix} J_{11} & J_{12} \\ J_{21} & J_{22} \end{bmatrix} \tag{61}$$

https://doi.org/10.1017/S0263574718000930 Published online by Cambridge University Press

Table I. Nominal parameters of two-link robot manipulator[1].

Parameters	Description	Value	Unit
m_1	Mass of link 1	2.0	kg
m_2	Mass of link 2	0.85	kg
l_1	Length of link 1	0.35	m
l_2	Length of link 2	0.31	m
I_1	Inertia of link 1	61.25×10^{-3}	kg m^2
I_2	Inertia of link 2	20.42×10^{-3}	kg m^2

Table II. Actual parameters of two-link robot manipulator.

Parameters	Description	Value	Unit
m_1	Mass of link 1	2.1	kg
m_2	Mass of link 2	1	kg
l_1	Length of link 1	0.35	m
l_2	Length of link 2	0.31	m
I_1	Inertia of link 1	0.01	kg m^2
I_2	Inertia of link 2	0.05	kg m^2

where

$$\begin{aligned} J_{11} &= -l_1 \sin(q_1) + l_2 \sin(q_1 + q_2) \\ J_{12} &= -l_2 \sin(q_1 + q_2) \\ J_{21} &= l_1 \cos(q_1) + l_2 \cos(q_1 + q_2) \\ J_{22} &= l_2 \cos(q_1 + q_2) \end{aligned} \tag{62}$$

Table I shows the nominal parameters of the robot dynamics of two-link manipulators. In this work, the link mass m_i and the inertia of the link l_i are assumed to be uncertain, as shown in Table II. The main factors affecting the uncertainty problems include loading, design or manufacturing errors, the life cycle of mechanical parts, assembly defects or using materials with poor qualities and so on.

The commanded trajectory chosen as circle x_{vd} in the free space is as follows:

$$x_{vd} = \begin{bmatrix} x_{vd1} \\ x_{vd2} \end{bmatrix} = \begin{bmatrix} 0.2 - 0.2\cos(\pi t) \\ 0.2 + 0.2\sin(\pi t) \end{bmatrix} \tag{63}$$

The radius circle is 0.2 and the center is located at $x = [0.2 \quad 0.2]^{\mathrm{T}}$. The wall is located at $x_e = 0.2$ m and has a nonlinear spring damper $F_x = 10,000(x - x_e)^2$. Due to the wall position, the end-effector tracks circle x_{vd} in the free space and moves slides along the wall when it contacts the wall. It is assumed that the robot manipulator dynamic (5) in Cartesian space interacts with a vertical wall shown in Fig. 3. The H vector consists of two uncertainty and disturbance terms, i.e., $\mathrm{H} = [H_x \; H_y]$, along x and y axes, respectively. Accordingly, two SRWNNs $i = 1, 2$ are applied to estimate H_x and H_y. The initial conditions are set to be $q(0) = [\frac{\pi}{2} \; -\frac{\pi}{6}]^{\mathrm{T}}$ and $\dot{q}(0) = [0 \; 0]^{\mathrm{T}}$.

Let the target impedance parameters be as follows:

$$\begin{aligned} M_m &= \mathrm{diag}[1.0] \qquad B_m = \mathrm{diag}[600.0] \\ K_m &= \mathrm{diag}[100.0] \end{aligned} \tag{64}$$

Remark 3. To prevent large sudden variations of torque motor signals, because of the large initial error in the transient response of the system, the gains of controllers K_1 and K_2 are increased linearly with time and arrive at the final value $K_1 = 50$ and $K_2 = 50$ after 1 s. Therefore, the transient responses of the torque control signals have desired behavior without large and sudden variations.

We consider four cases for the simulation. In cases 1 and 2, feedback linearization control and dynamic surface are considered, respectively. The purpose of the simulation in cases 1 and 2 is to

https://doi.org/10.1017/S0263574718000930 Published online by Cambridge University Press

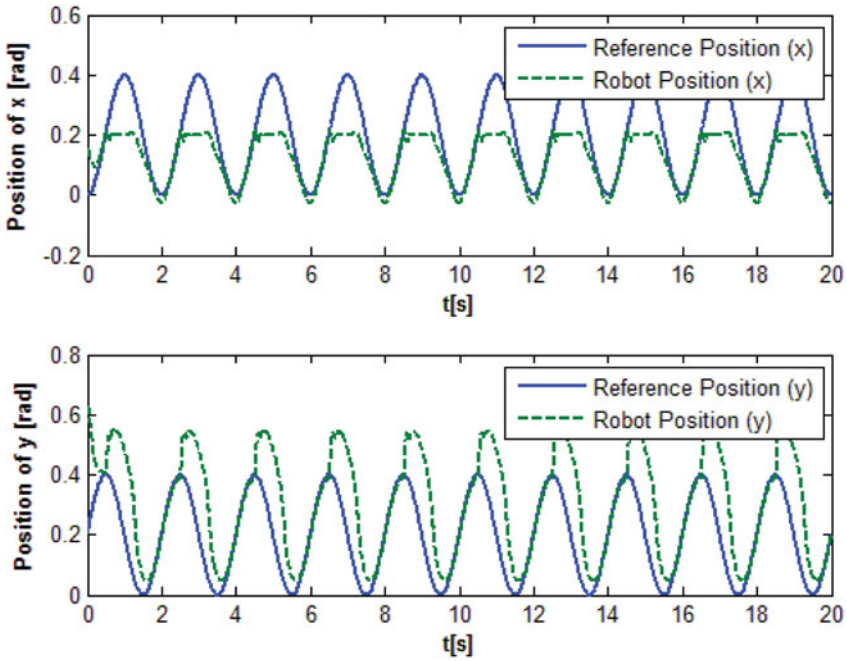


Fig. 4. Position tracking with feedback linearization control (case 1).

compare the performance of two mentioned nonlinear methods based on the uncertainties mentioned in Table II. In case 2, according to Eq. (37), term $\hat{H}(x)$ is only including the uncertainties. In fact, adaptive law (38) and the entire NN have been omitted. In cases 3 and 4, the dynamic surface method and proposed adaptive controller are studied by considering the various uncertainties and disturbances. In case 3, according to Eq. (37), term $\hat{H}(x)$ is including both the uncertainties and disturbances. In addition, adaptive law (38) is not considered. Finally, in case 4, the proposed adaptive law (38) is applied to remove the uncertainties and disturbances term $\hat{H}(x)$.

4.1. Case 1: feedback linearization

Initially, we examine feedback linearization control. The control performance is studied without considering the adaptive rule (38). Figures 4–6 show the position tracking of the robot, tracking errors and control torques, respectively. From the simulation results, it can be concluded that feedback linearization control has large tracking errors, especially in the y position. It is obvious from Fig. 3 that, because of the wall position, the end-effector tracks circle x_d and moves slides along the wall when it contacts the wall. Consequently, according to Fig. 5, the wall position and the definition of commanded trajectory x_{vd} lead to observe the large error value of the x position, which can be considered as a normal operation. Therefore, it is normal to observe this error. From Fig. 6, it can be observed that the torque motor signals have large sudden variations, which can decrease the life cycle of the actuators and damage them.

4.2. Case 2: dynamic surface impedance control (DSIC)

To show the performance of DSIC, we study the DSIC performance without considering disturbance and model uncertainties. The position tracking and the errors are depicted in Figs. 7 and 8. In addition, control signals are plotted in Fig. 9. As can be observed from the results, the tracking errors and the value of control torque have been improved as compared to feedback linearization control. In fact, based on Eq. (43), K_2 gain in the DSIC decreases the effects of the uncertainties terms mentioned in Table II and improves the tracking errors and control signals.

https://doi.org/10.1017/S0263574718000930 Published online by Cambridge University Press

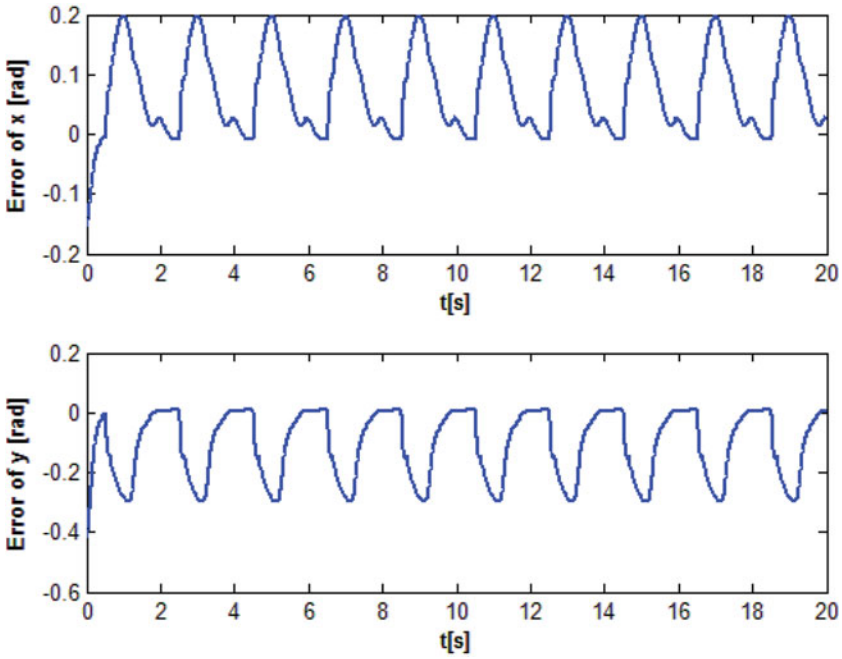


Fig. 5. Tracking errors with feedback linearization control (case 1).

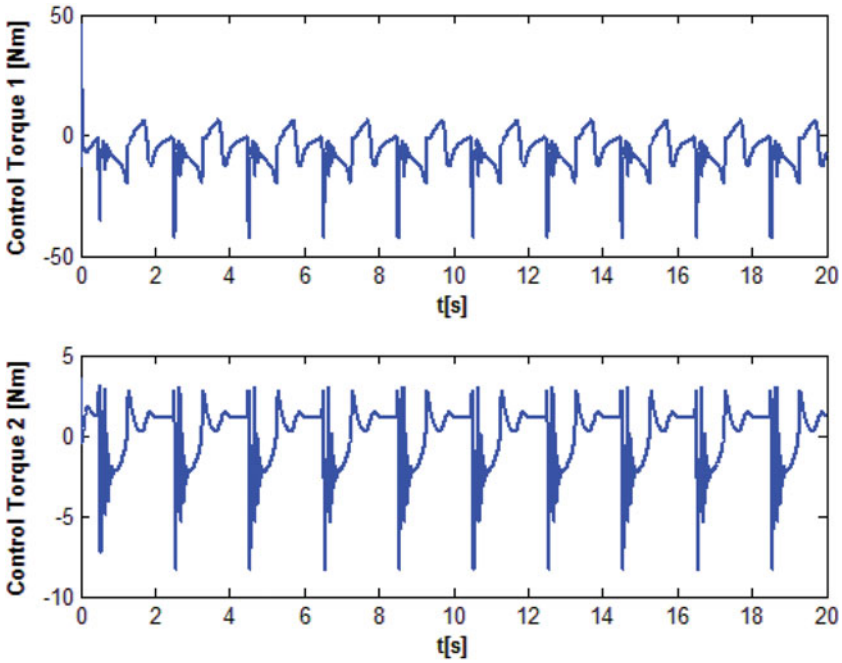


Fig. 6. Control signals with feedback linearization control (case 1).

4.3. Case 3: dynamic surface impedance control with uncertainties and disturbances

We know only the value of the nominal parameters in Table I and design a controller based on the known parameters. Additionally, the fixed external disturbance $\hat{F}_1$ is given by

$$\hat{F}_1 = \begin{cases} \begin{bmatrix} 68 & 68 \end{bmatrix}^{\mathrm{T}}, & t \geq 7\,\mathrm{s} \\ \begin{bmatrix} 0 & 0 \end{bmatrix}^{\mathrm{T}}, & t < 7\,\mathrm{s} \end{cases} \tag{65}$$

https://doi.org/10.1017/S0263574718000930 Published online by Cambridge University Press

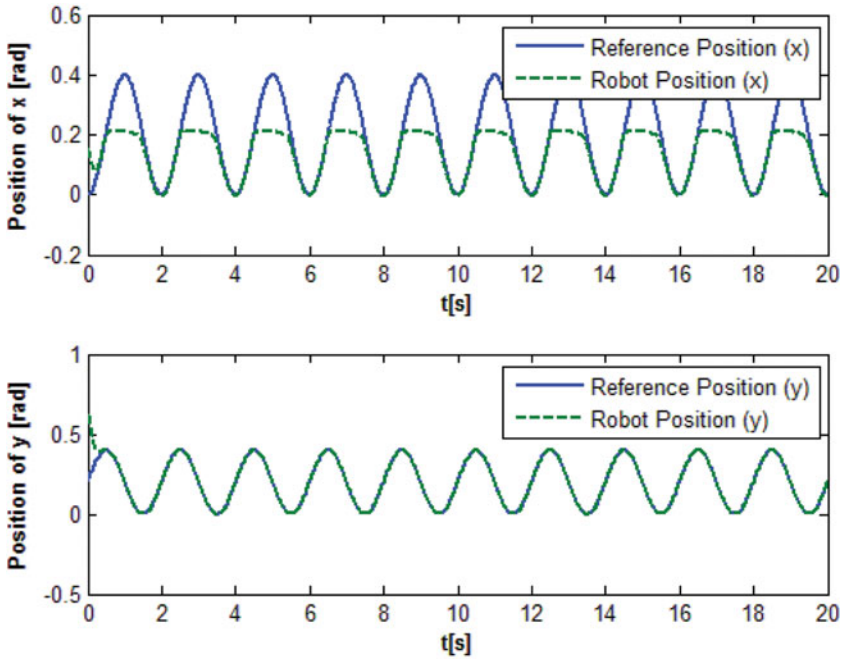


Fig. 7. Position tracking with DSIC (case 2).

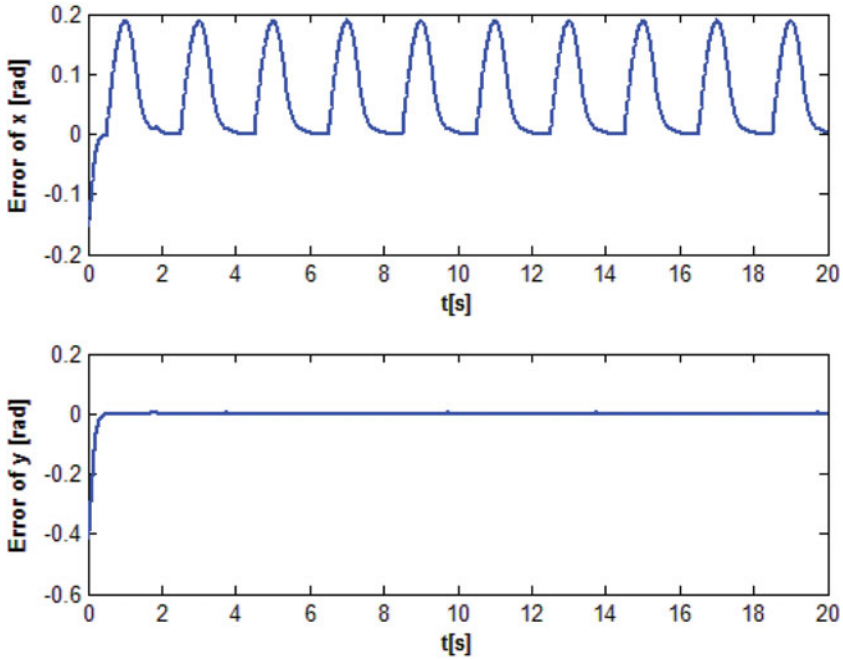


Fig. 8. Tracking errors with DSIC (case 2).

To demonstrate that the proposed control (37) has the ability to remove the nonlinear disturbance dynamic, we consider time variant disturbance $\hat{F}_2$ as follows:

$$\hat{F}_2 = \begin{cases} \begin{bmatrix} 68 & 68\sin(t) \end{bmatrix}^{\mathrm{T}}, & t \geq 7\,\mathrm{s} \\ \begin{bmatrix} 0 & 0 \end{bmatrix}^{\mathrm{T}}, & t < 7\,\mathrm{s} \end{cases} \tag{66}$$

Now, according to Table II, to simulate, we consider the disturbances (65) and (66) separately and uncertainty. Figures 10–12 show the position tracking, errors and control signal responses of

https://doi.org/10.1017/S0263574718000930 Published online by Cambridge University Press

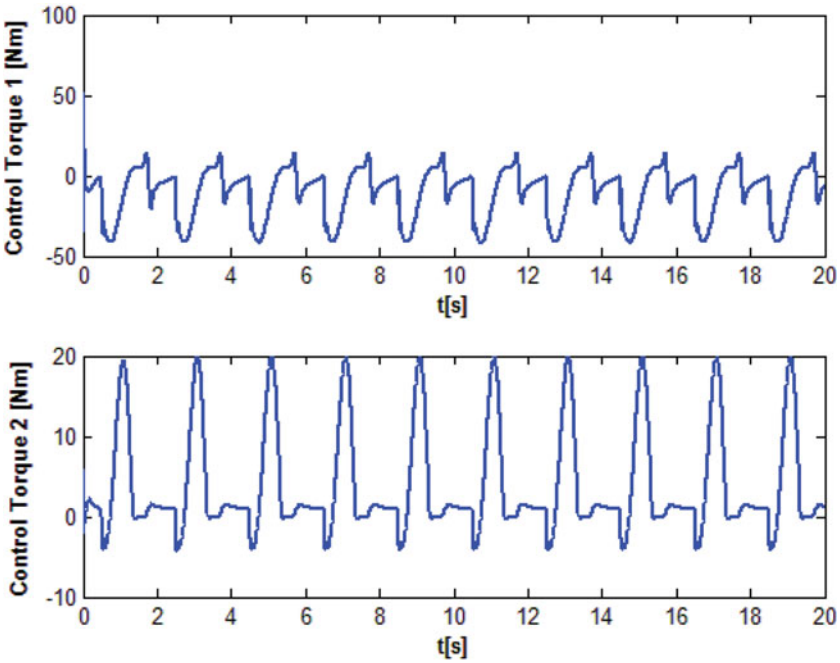


Fig. 9. Control signals with DSIC (case 2).

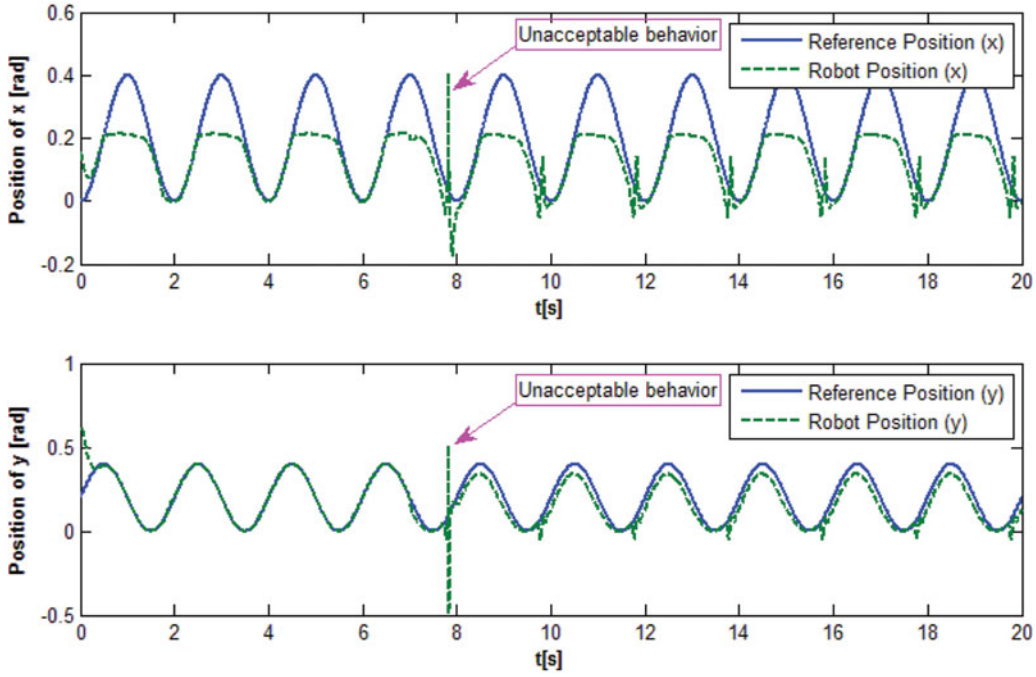


Fig. 10. Position tracking with DSIC in the presence of the uncertainty and disturbance $\hat{F}_1$ (case 3).

disturbance (65), respectively. Figures 13–15 depict the position tracking, errors and control signal responses of disturbance (66). Figures 10 and 13 show the sudden and large deviation from the desired trajectory as an unacceptable behavior in the position tracking. It can be observed from Figures 12 and 15 that the magnitude control torque signals are too large, and disturbances and uncertainties also lead to saturate actuators. That is, the process control is failed because the actuators are not able to produce such a large torque.

https://doi.org/10.1017/S0263574718000930 Published online by Cambridge University Press

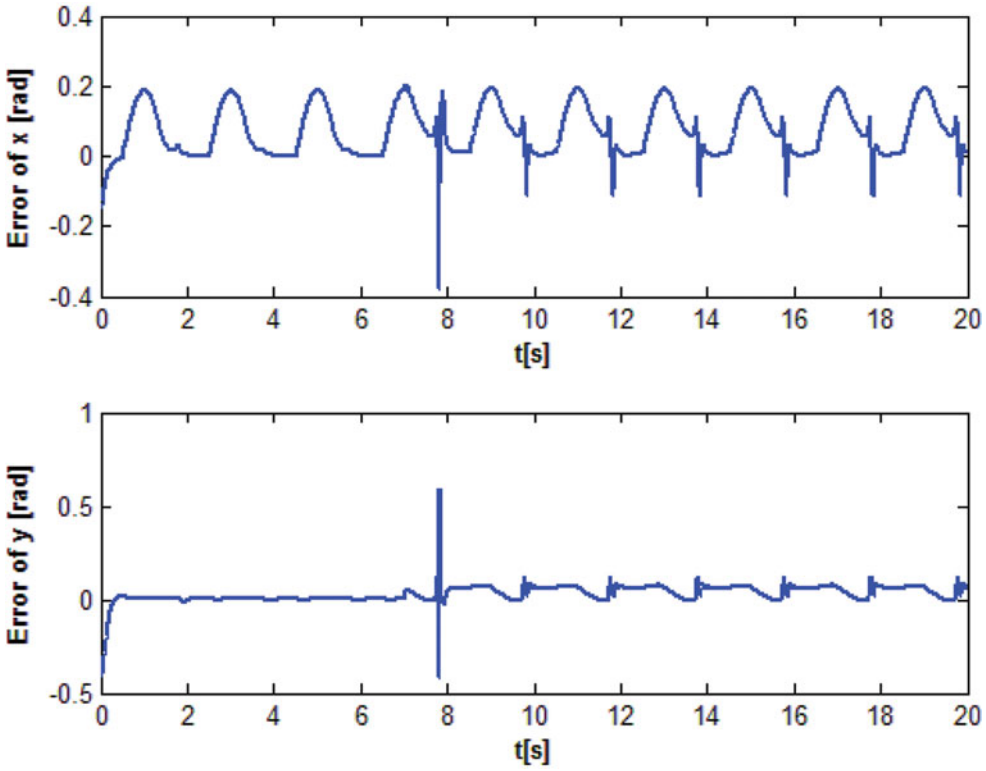


Fig. 11. Tracking errors with DSIC in the presence of the uncertainty and disturbance $\hat{F}_1$ (case 3).

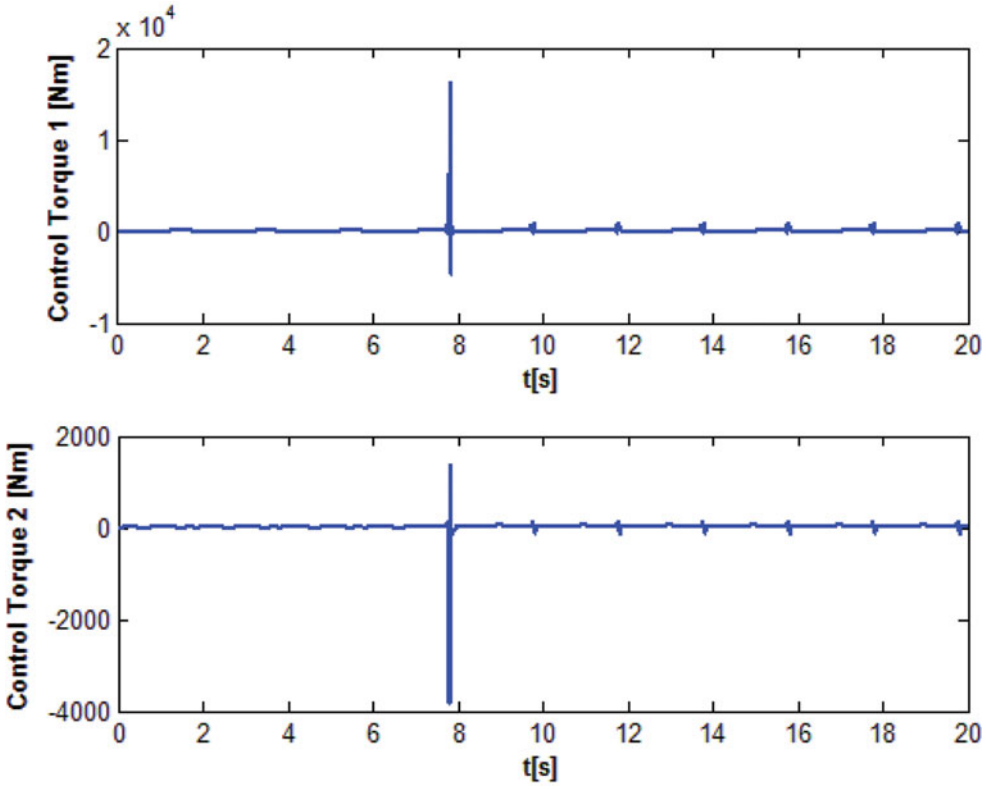


Fig. 12. Control signals with DSIC in the presence of the uncertainty and disturbance $\hat{F}_1$ (case 3).

https://doi.org/10.1017/S0263574718000930 Published online by Cambridge University Press

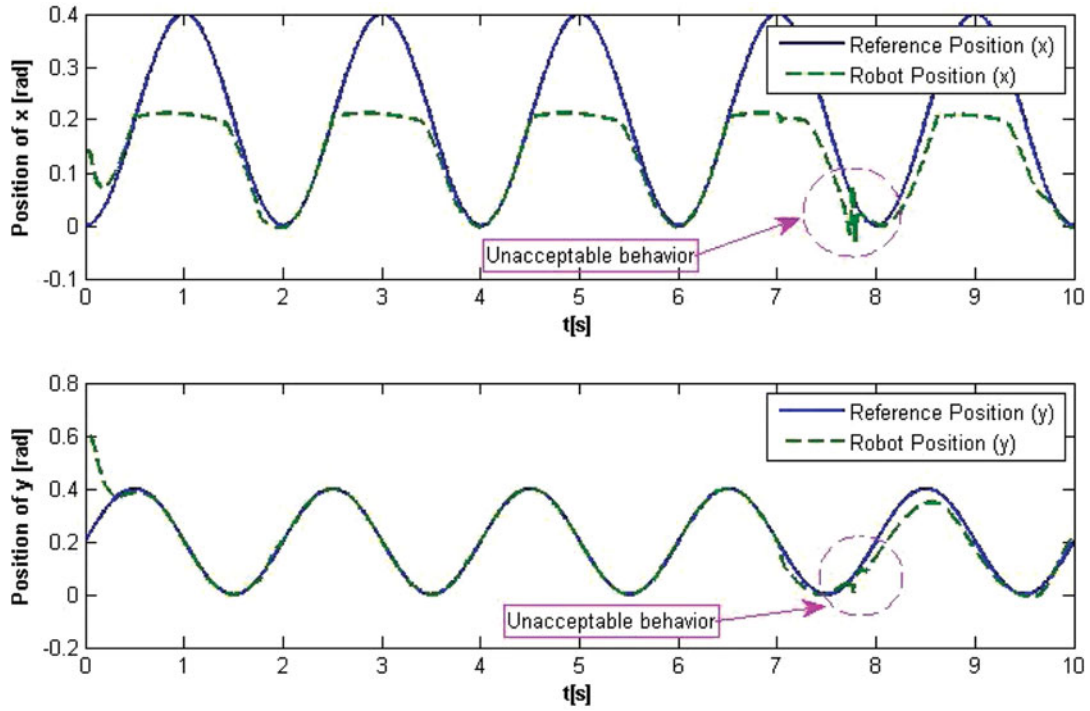


Fig. 13. Position tracking with DSIC in the presence of the uncertainty and disturbance $\hat{F}_2$ (case 3).

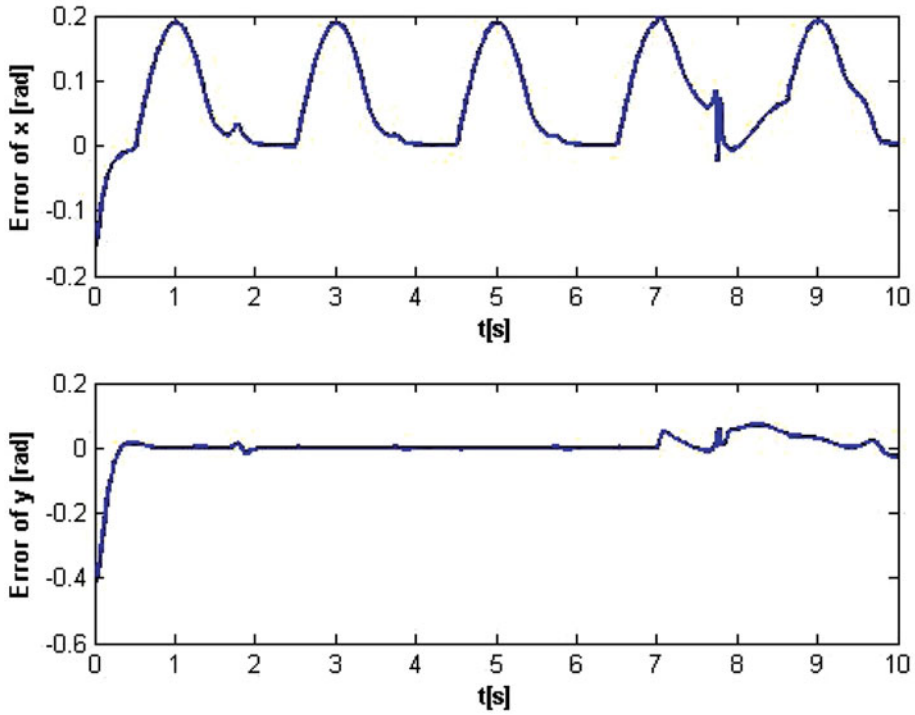


Fig. 14. Tracking errors with DSIC in the presence of the uncertainty and disturbance $\hat{F}_2$ (case 3).

https://doi.org/10.1017/S0263574718000930 Published online by Cambridge University Press

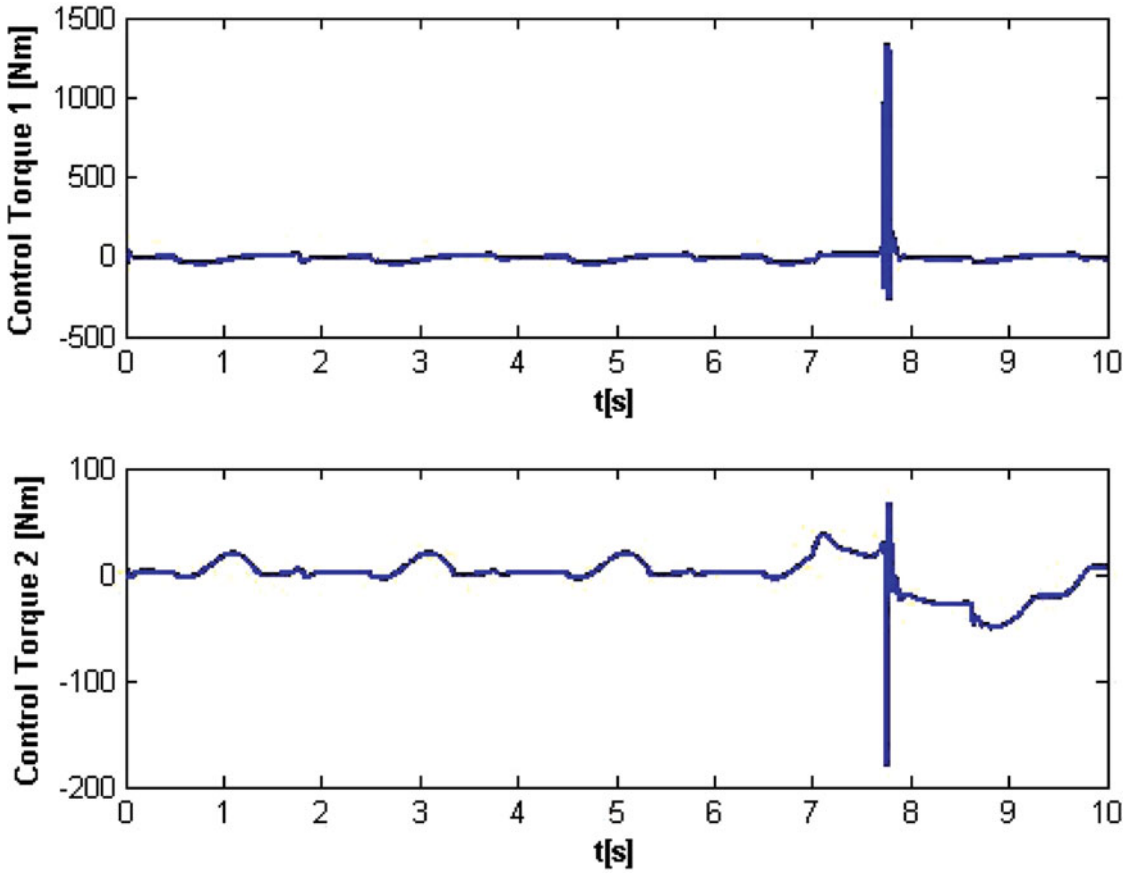


Fig. 15. Control signals with DSIC in the presence of the uncertainty and disturbance $\hat{F}_2$ (case 3).

4.4. Case 4: adaptive dynamic surface impedance control with uncertainties and disturbances

In this case, we demonstrate the effectiveness of the proposed ADSI controller Theorem 1 to handle unknown model parameters and remove the saturation effect. The Control signals are restricted inbound of $-60N.m.$ and $+60N.m.$ In fact, saturation bounds are selected based on the ability of the actuators in order to apply control signals to force the robot for tracking the desired trajectory. In this simulation, due to lightweight and structure of the robot (Table 1), we considered that the installed actuators of the robot are not very powerful to prepare the control signals bigger than the mentioned bounded. Controller parameters for the SRWNN-based adaptive DSIC are chosen as $\mu = diag[1.0\ 1.0]$, $\kappa = 0.005$ and $\tau_2 = 0.005$. We employ two SRWNNs, each of which has 5 wavelones. The initial values of the parameters are given randomly between 0 and 1. We consider the multi-dimensional wavelet neural network. In this case, the input is a multidimensional vector and the wavelones consist of the multidimensional wavelet activation functions. Because of considering the planner two-dimensional manipulator in the simulation sections, we consider two separated neural networks to estimate the disturbances and uncertainties in the directions of the x, y. The wavelone parameters include dilation and translation coefficients. The structure of the SRWNN to estimate uncertainty and disturbances for H_x are shown in the Fig. 16. It is worth noting that the structure of the SRWNN for estimation of the H_y is same as Fig. 16. $x = [x_1 \dots x_8]^T = [q_1\ \dot{q}_1\ q_2\ \dot{q}_2\ q_{ref1}\ \dot{q}_{ref1}\ q_{ref2}\ \dot{q}_{ref2}]$ is the input of the network. In addition, u_j and φ_j where $j = 1 \dots 5$ are considered as inputs and outputs of the wavelones, respectively.

https://doi.org/10.1017/S0263574718000930 Published online by Cambridge University Press

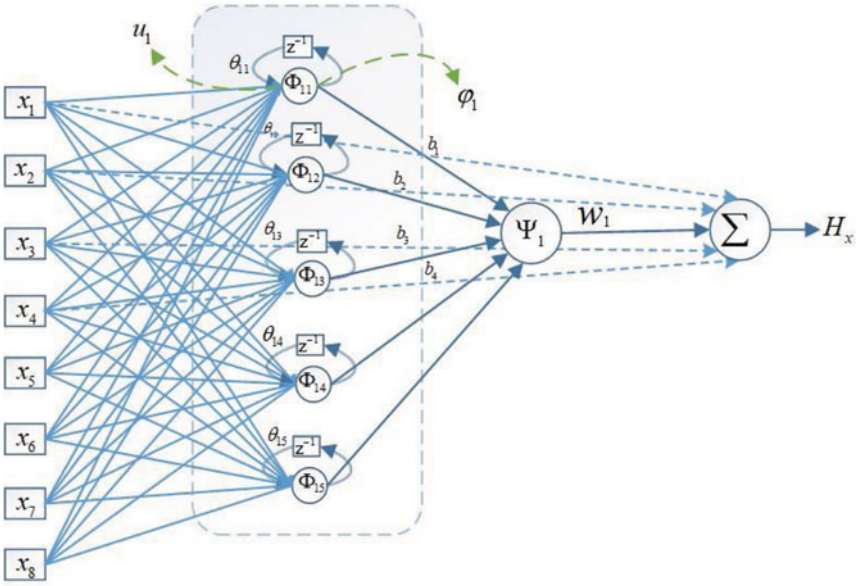


Fig. 16. The structure of the SRWNN to estimate uncertainty and disturbances of H_x.

To explain more in detail, we can consider the performance of the first wavelone as follows:

$$u_1(n) = x_i(n) + \theta_i \phi_i(n-1) \tag{67}$$

$$z_i(n) = \frac{u_1(n) - m_i}{d_i} \tag{68}$$

$$\phi_i = -z_i * \exp\left(-\frac{1}{2} * z_i^2\right) \tag{69}$$

where $i = 1 \ldots 8$ is the number of the network input, u_1 is the input of the first wavelone, m_i is translation, d_i is dilation coefficients, z_i is the input of the activation function, ϕ_i is the activation function that the first derivative of Gaussian function, i.e. $\phi(x) = (-x)e^{-\frac{1}{2}x^2}$, is used as the mother-wavelet. Eventually, the output of the first wavelone is:

$$\varphi_1 = \prod_{i=1}^{8} \phi_i \tag{70}$$

φ_1 is the output of the first wavelone. One can refer to section 3.2 for more details.

Fig. 17 and Fig. 20 depict acceptable position tracking of the robot while the robot manipulator has a negligible deviation from the desired trajectory. It is obvious from Fig. 18 and Fig. 21 that tracking errors are acceptable and lessened in comparison to case 3. The proposed ADSI controller is able to handle disturbances and unknown dynamics; while position tracking of x and y has a smooth and acceptable behavior with respect to Fig. 10 and Fig. 13. It is worth mentioning that although the uncertainties and disturbances are not removed from the systems, based on the Eqs. (65-66) and Table 2, the robot is able to track the desired trajectory with acceptable performance and the position tracking errors are negligible.

According to Fig. 12 and Fig. 15, in presence of uncertainties and disturbances, the amplitude of the control torque signals is too large. From Fig. 18, Fig. 21 and as a practical implementation point of view, the proposed adaptive controller is able to remove uncertainties and disturbances as one of the sources of the actuator saturation. It can be observed from Fig. 19 and Fig. 22, the proposed controller is able to apply the proper control signals in order to remove the uncertainties and disturbances (65) and (66).

https://doi.org/10.1017/S0263574718000930 Published online by Cambridge University Press

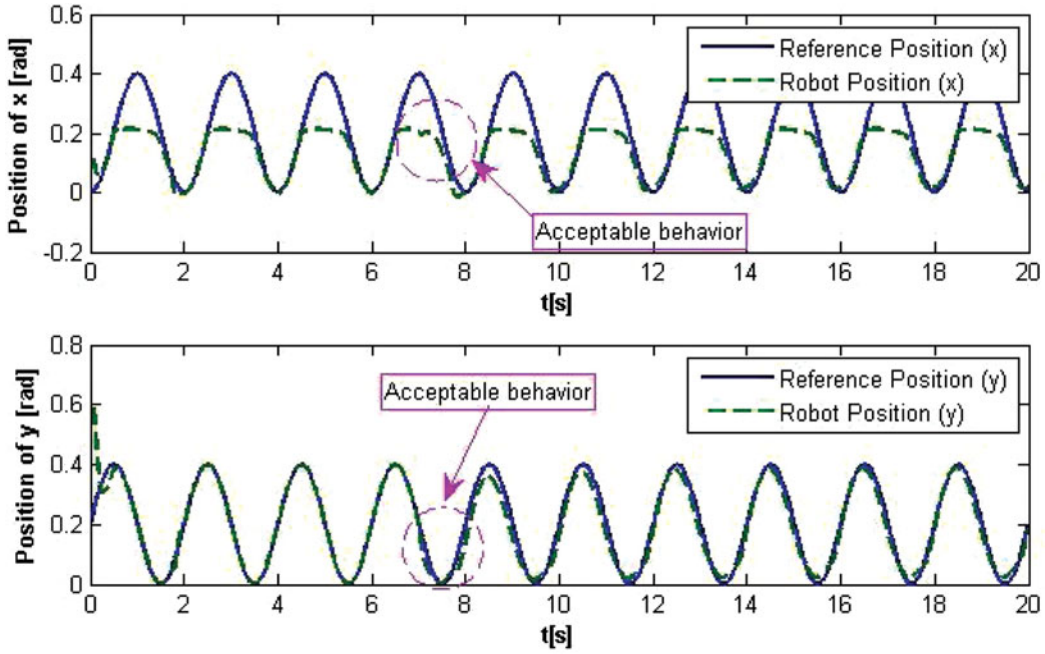


Fig. 17. Position tracking with the ADSI controller in the presence of the uncertainty and disturbance $\hat{F}_1$ (case 4).

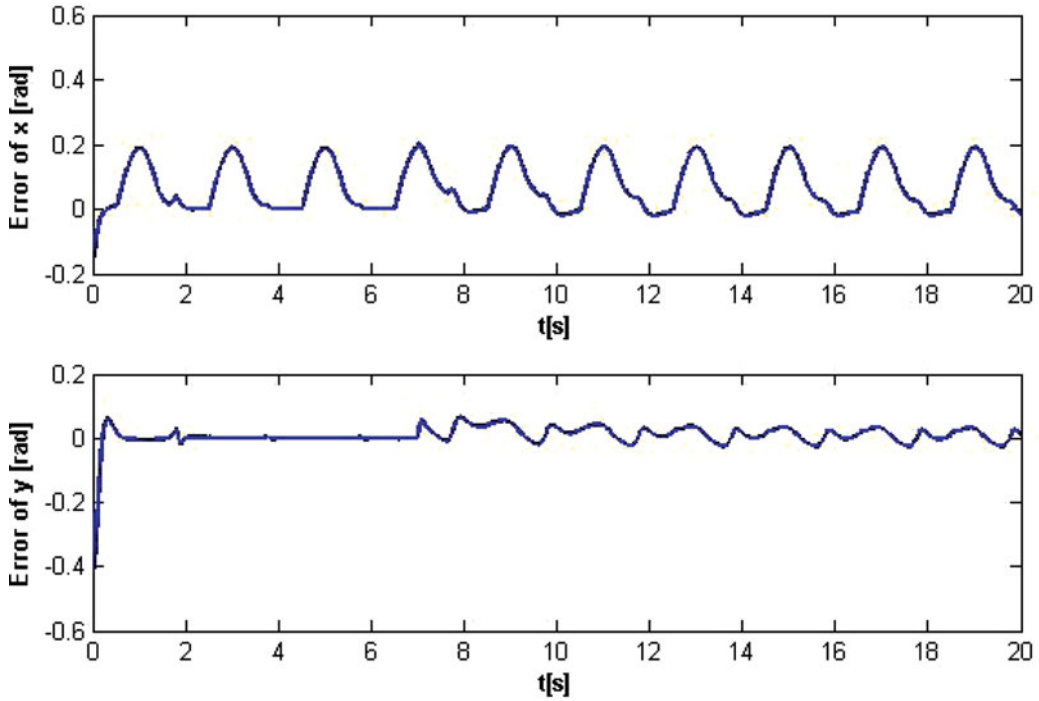


Fig. 18. Tracking errors with the ADSI controller in the presence of the uncertainty and disturbance $\hat{F}_1$ (case 4).

https://doi.org/10.1017/S0263574718000930 Published online by Cambridge University Press

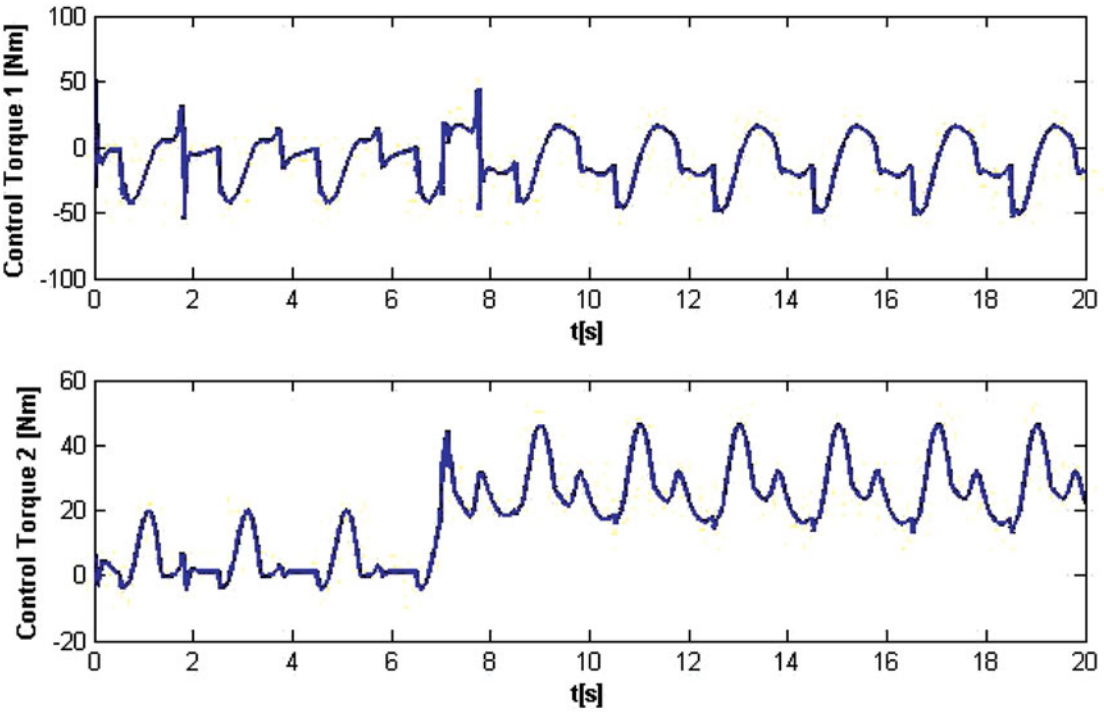


Fig. 19. Control signals with the ADSI controller in the presence of the uncertainty and disturbance $\hat{F}_1$ (case 4).

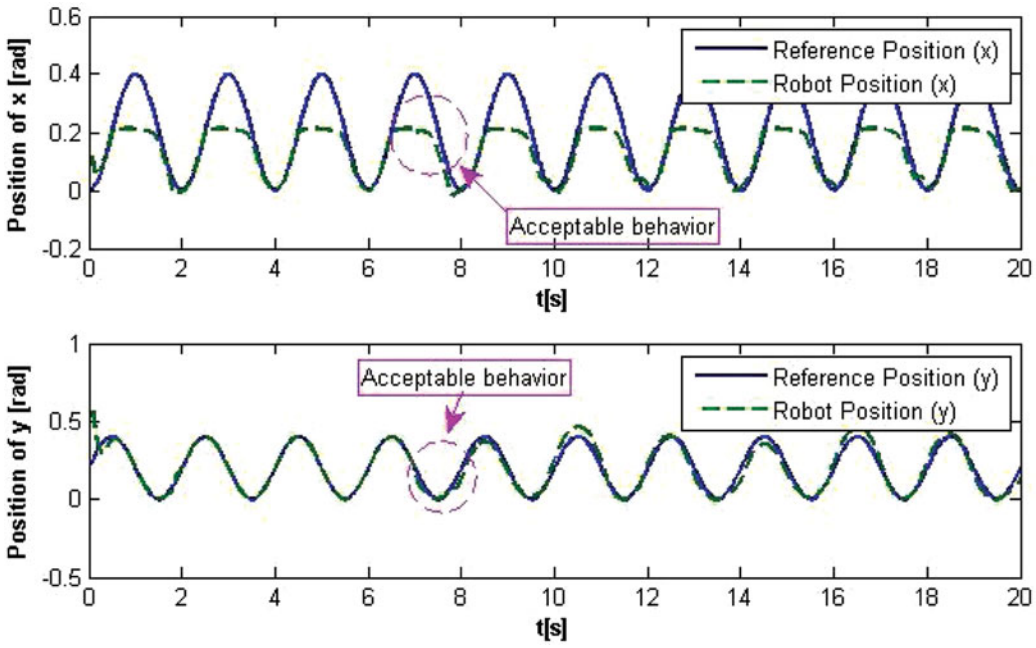


Fig. 20. Position tracking with the ADSI controller in the presence of the uncertainty and disturbance $\hat{F}_2$ (case 4).

https://doi.org/10.1017/S0263574718000930 Published online by Cambridge University Press

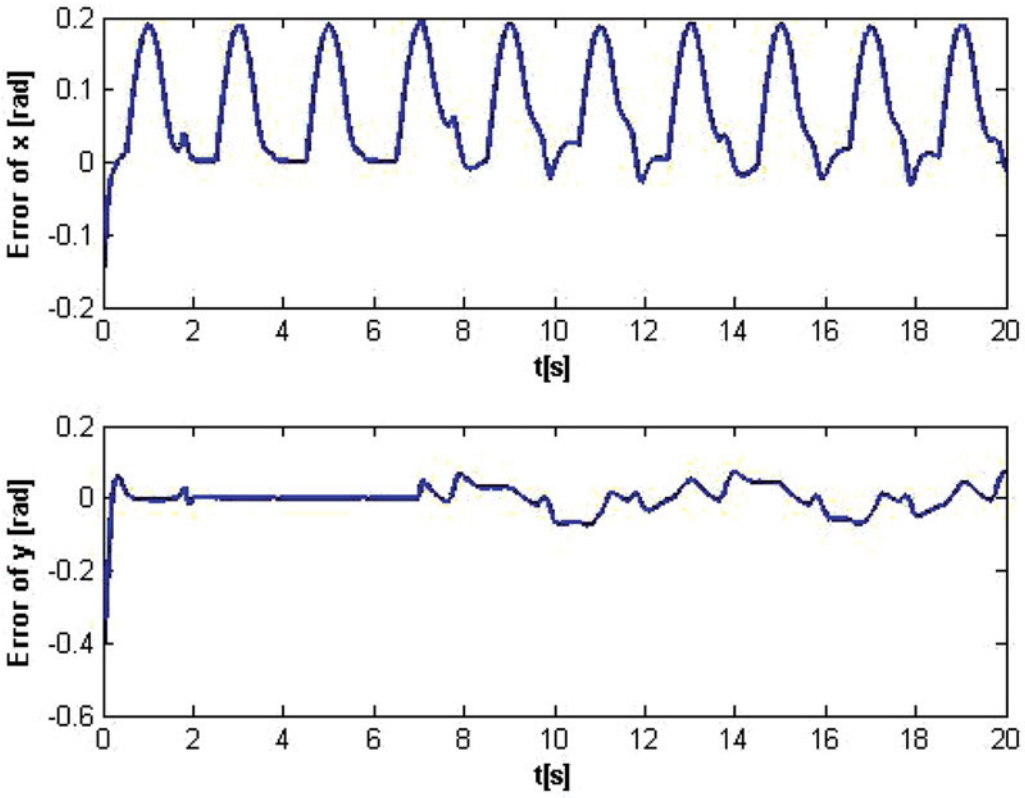


Fig. 21. Tracking errors with the ADSI controller in the presence of the uncertainty and disturbance $\hat{F}_2$ (case 4).

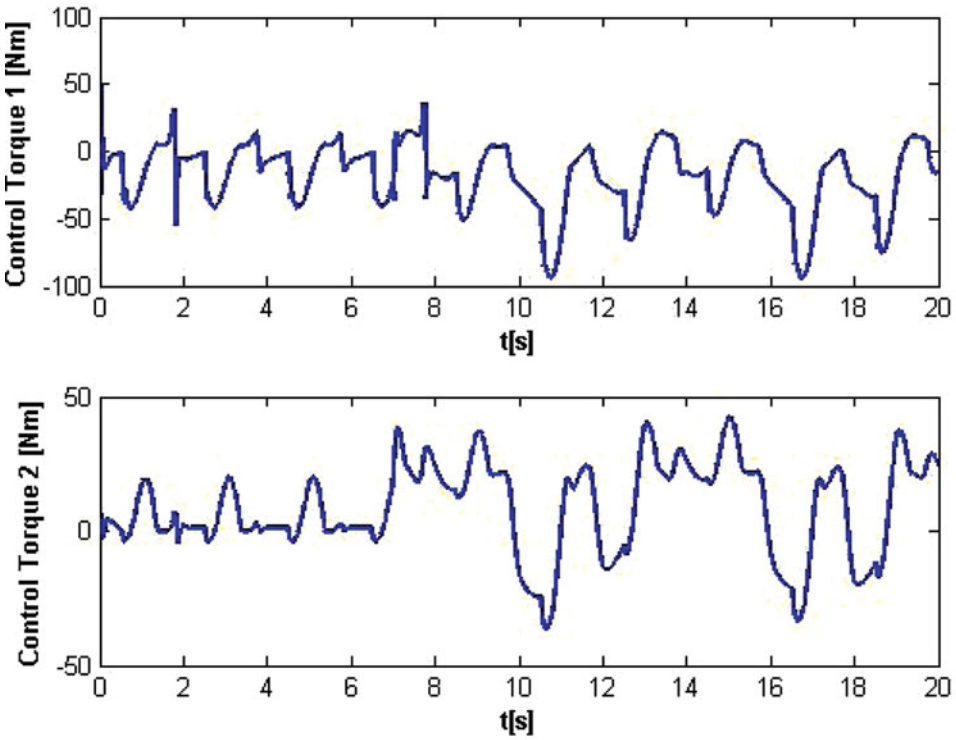


Fig. 22. Control signals with the ADSI controller in the presence of the uncertainty and disturbance $\hat{F}_2$ (case 4).

https://doi.org/10.1017/S0263574718000930 Published online by Cambridge University Press

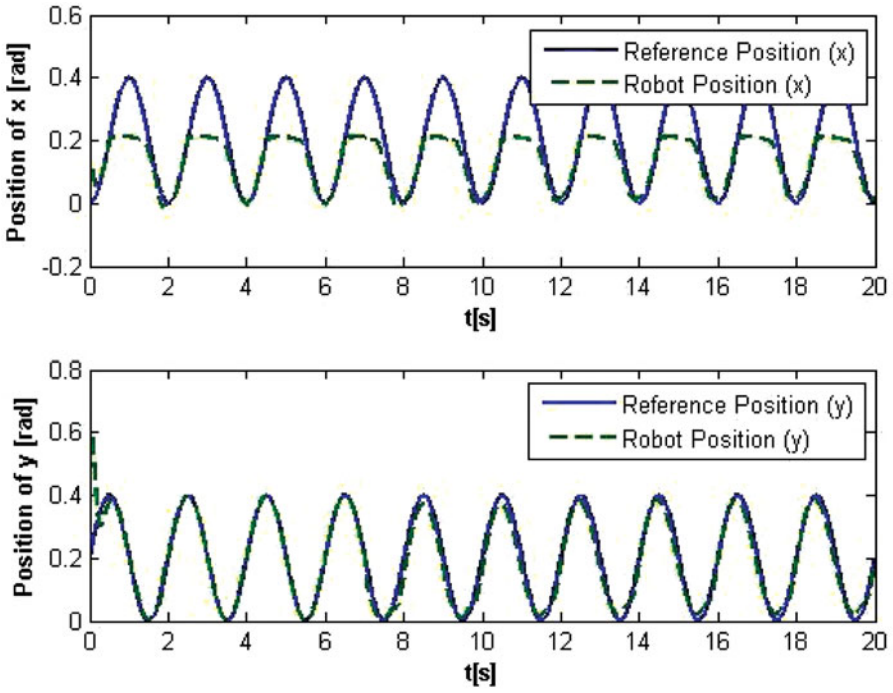


Fig. 23. Tracking position with the ADSI controller in the presence of the uncertainty and disturbance $\hat{F}_3$ (case 4).

Now, to show the ability of the proposed adaptive law (38) to remove uncertainties and disturbances with a fast convergence rate, we apply both disturbances (65) and (66) to the system as the following structure:

$$\hat{F}_3 = \begin{cases} \left[68\ 68\sin(t)\right]^{\mathrm{T}}, & 7 \le t < 9\,\mathrm{s} \\ \left[68\ 68\right]^{\mathrm{T}}, & t \ge 9\,\mathrm{s} \end{cases} \tag{71}$$

The main properties of disturbances (71) are that they can simultaneously evaluate the proposed control system ability in the presence of two different disturbances (fixed and time variant structures). Figures 23 and 24 depict the position tracking and tracking errors of the robots in the presence of disturbance (71) and uncertainty according to Table II. Although two disturbances (65) and (66) are applied to the system, the proposed adaptive law is able to remove them with fast convergence to adapt its parameters, while the control signals are bounded between -60 N m and $+60$ N m (Fig. 25).

Table III provides the root mean square (RMS) of the position errors and torque control signals of cases 3 and 4. This reveals that proposed controller (ADSI) improves the performance of the systems by decreasing the position errors (RMS) and the magnitude of the torque control signals (RMS).

5. Conclusion

In this paper, we have considered the combination of the dynamic surface approach and SRWNN to solve the impedance control problem and make a robust control system to overcome the saturation effect of the n-link robot manipulators. DSC is applied to force the robot manipulator to have desired impedance and SRWNNs with self-feedback neurons, which are used to approximate the dynamic parametric uncertainties and external disturbances. Formulated target impedance in the state–space and defined effective dynamic surface errors lead to obtain a simple structure to track the desired impedance. Based on the ADSI controller, the robot manipulator tracks the desired impedance and is robust against both parametric uncertainties and external disturbances. Adaptation laws for training parameters of SRWNNs were obtained in the sense of Lyapunov approach. Uniformly ultimately bounded stability of the closed-loop system has been verified using Lyapunov's direct method. In

https://doi.org/10.1017/S0263574718000930 Published online by Cambridge University Press

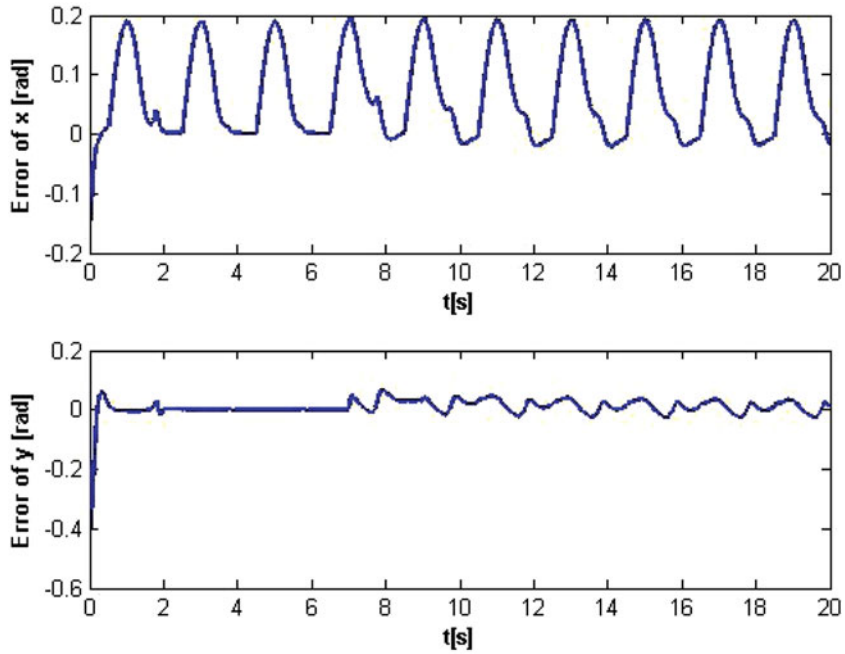


Fig. 24. Tracking errors with the ADSI controller in the presence of the uncertainty and disturbance $\hat{F}_3$ (case 4).

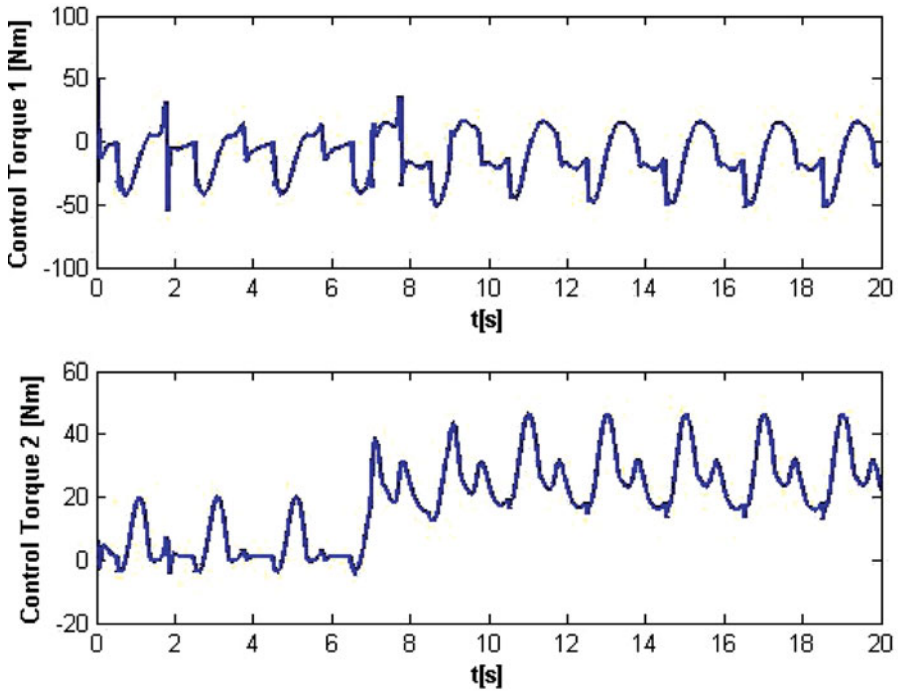


Fig. 25. Control signals with the ADSI controller in the presence of the uncertainty and disturbance $\hat{F}_3$ (case 4).

the simulation studies, the ability of the proposed controller to compensate the disturbance and uncertainty of the dynamic model parameters was monitored, and the results were compared with those of the DSIC without any adaptation laws. Simulation results verify that the proposed control law is able to track a target impedance model with good performance while control torque signals are acceptable.

https://doi.org/10.1017/S0263574718000930 Published online by Cambridge University Press

Table III. RMS of the position errors and control signals of cases 3 and 4.

Signal Controller	Position error X (RMS)	Position error Y (RMS)	Control signal X (RMS)	Control signal Y (RMS)
DSIC in the presence of the uncertainty and disturbance $\hat{F}_1$ (case 3)	0.1021	0.0575	417.0722	100.9088
Proposed ADSI in the presence of the uncertainty and disturbance $\hat{F}_1$ (case 4)	0.0977	0.0358	22.3077	23.3161
DSIC in the presence of the uncertainty and disturbance $\hat{F}_2$ (case 3)	0.0990	0.0474	80.4216	18.0303
Proposed ADSI in the presence of the uncertainty and disturbance $\hat{F}_2$ (case 4)	0.0975	0.0421	30.9284	18.9639
Proposed ADSI in the presence of the uncertainty and disturbance $\hat{F}_3$ (case 4)	0.0977	0.0353	22.6018	22.8972

References

1. W. He, Y. Dong and C. Sun, "Adaptive neural impedance control of a robotic manipulator with input saturation," *IEEE Trans. Syst., Man, Cybern., Syst.* **46**(3), 334–344 (2016).
2. N. Hogan, "Impedance control: An approach to manipulation. Part I: Theory; Part II: Implementation; Part III: Applications," *J. Dyn. Syst. Meas. Control* **107**(1), 8–16 (1985).
3. S. P. Chan, B. Yao, W. B. Gao and M. Cheng, "Robust Impedance control of robot manipulators," *Int. J. Robot. Autom.* **6**(4), 220–227 (1991).
4. C. Canudas de Wit, B. Siciliano and G. Bastin (Eds), *Theory of Robot Control* (Springer-Verlag, London, 1996), ISBN-13:978-1-4471-1503-8.
5. J. J.-B. Mvogo Ahanda, J. B. Mbede, A. Melingui and B. Essimbi, "Robust adaptive control for robot manipulators: Support vector regression-based command filtered adaptive backstepping approach," *Robotica* **36**, 516–532 (2018).
6. J. H. Oh and J. S. Lee, "Control of Flexible Joint Robot System by Backstepping Design Approach," *Proceedings of the* IEEE Int*ernational* Con*ference on Robotics and* Autom*ation* (1997) pp. 3435–3440.
7. S.-C. Tong and Y.-M. Li, "Adaptive fuzzy output feedback tracking backstepping control of strict-feedback nonlinear systems with unknown deadzones," *IEEE Trans. Fuzzy Syst.* **20**(1), 168–180 (2012).
8. C. Kwan and F. L. Lewis, "Robust backstepping control of nonlinear systems using neural networks," *IEEE Trans. Syst., Man, Cybern. A, Syst., Humans* **30**(6), 753–766 (Nov. 2000).
9. D. Swaroop, J. K. Hedrick, P. P. Yip and J. C. Gerdes, "Dynamic surface control for a class of nonlinear systems," *IEEE Trans. Autom. Control* **45**(10), 1893–1899 (2000).
10. P. P. Yip and J. K. Hedrick, "Adaptive dynamic surface control: A simplified algorithm for adaptive backstepping control of nonlinear systems," *Int. J. Control* **71**(5), 959–979 (1998).
11. D. Wang and J. Huang, "Neural network-based adaptive dynamic surface control for a class of uncertain nonlinear systems in strict-feedback form," *IEEE Trans. Neural Netw.* **16**(1), 195–202 (2005).
12. Y. H. Kim and F. L. Lewis, "Reinforcement adaptive learning neural-net based friction compensation control for high speed and precision," *IEEE Trans. Control Syst. Technol.* **8**(1), 118–126 (2000).
13. B. Xu, "Robust adaptive neural control of flexible hypersonic flight vehicle with dead-zone input nonlinearity," *Nonlin. Dyn.* **80**(3), 1509–1520 (2015).
14. M.-C. Chien and A.-C. Huang, "Adaptive impedance control of robust manipulators based on function approximation technique," *Robotica* **22**(4), 395–403 (2004).
15. R. Kamnik, D. Matko and T. Bajd, "Application of model reference adaptive control to industrial robot impedance control," *J. Intell. Robot. Syst.* **22**(2), 153–163 (1998).
16. C. Cheah and D.-W. Wang, "Learning impedance control for robotic manipulators," *IEEE Trans. Robot. Autom.* **14**(3), 452–465 (1998).
17. W.-S. Lu and Q.-H. Meng, "Impedance control with adaptation for robotic manipulations," *IEEE Trans. Robot. Autom.* **7**(3), 408–415 (1991).
18. R. Colbaugh, H. Seraji and K. Glass, "Direct adaptive impedance control of robot manipulators," *J. Robot. Syst.* **10**(2), 217–248 (1993).
19. S. J. Yoo, J. B. Park and Y. H. Choi, "Adaptive dynamic surface control of flexible-joint robots using self-recurrent wavelet neural networks," *IEEE Trans. Syst., Man, Cybern., Syst.* **36**(6), 1342–1355 (2006).
20. M. Gaeta, V. Loia, F. Orciuoli and P. Ritrovato, "S-WOLF: Semantic workplace learning framework," *IEEE Trans. Syst., Man, Cybern., Syst.* **45**(1), 56–72 (2015).
21. Z. Li and C.-Y. Su, "Neural-adaptive control of single-master–multiple slaves teleoperation for coordinated multiple mobile manipulators with time-varying communication delays and input uncertainties," *IEEE Trans. Neural Netw. Learn. Syst.*, **24**(9), 1400–1413 (2013).
22. S.-L. Dai, C. Wang and F. Luo, "Identification and learning control of ocean surface ship using neural networks," *IEEE Trans. Ind. Inform.* **8**(4), 801–810 (2012).

https://doi.org/10.1017/S0263574718000930 Published online by Cambridge University Press

23. Z. Liu, C. Chen, Y. Zhang and C. L. P. Chen, "Adaptive neural control for dual-arm coordination of humanoid robot with unknown nonlinearities in output mechanism," *IEEE Trans. Cybern.* **45**(3), 521–532 (2015).
24. C. F. Hsu, C. M. Lin and R. G. Yeh, "Supervisory adaptive dynamic RBF-based neural fuzzy control system design for unknown nonlinear systems," *Appl. Soft Comput.* **13**, 1620–1626 (2013).
25. H. J. Rong, S. Han and G. S. Zhao, "Adaptive fuzzy control of aircraft wing-rock motion," *Appl. Soft Comput.* **14**, 181–193 (2013).
26. S. A. Mohamad Dehghan, M. Danesh, F. Sheikholeslam and M. Zekri, "Adaptive force–environment estimator for manipulators based on adaptive wavelet neural network," *Appl. Soft Comput.* **28**, 527–540 (2015).
27. M. Zekri, S. Sadri and F. Sheikholeslam, "Adaptive fuzzy wavelet network control design for nonlinear systems," *Fuzzy Sets Syst.* **159**, 2668–2695 (2008).
28. Q. Zhang and A. Benveniste, "Wavelet networks," *IEEE Trans. Neural Netw.* **3**(6), 889–898 (1992).
29. J. Zhang, G. Walter, Y. Miao and W. N. W. Lee, "Wavelet neural networks for function learning," *IEEE Trans. Signal Process.* **43**(6), 1485–1497 (1995).
30. Y. Oussar, I. Rivals, L. Personnaz and G. Dreyfus, "Training wavelet networks for nonlinear dynamic input–output modeling," *Neurocomputing* 20(1-3), 173–188 (1998).
31. B. R. Bakshi and G. Stephanopoulos, "Wave-net: A multiresolution, hierarchical neural network with localized learning," *AIChE J.* **39**(1), 57–81 (1993).
32. O. Rioul and M. Vetterli, "Wavelets and signal processing," *IEEE Signal Process. Mag.* **8**(4), 14–38 (1991).
33. F. J. Lin, H. J. Shieh, P. H. Shieh and P. H. Shen, "An adaptive recurrent neural-network motion controller for X–Y table in CNC machine," *IEEE Trans. Syst., Man, Cybern. B, Cybern.* **36**(2), 286–299 (2006).
34. C. M. Lin and C. F. Hsu, "Recurrent-neural-network-based adaptive backstepping control for induction servomotors," *IEEE Trans. Ind. Electron.* **52**(6), 1677–1684 (2005).
35. S. J. Yoo, Y. H. Choi and J. B. Park, "Identification of dynamic systems using a self-recurrent wavelet neural network: Convergence analysis via adaptive learning rates," *J. Control Autom. Syst.* **11**(9), 781–788 (2005).
36. S. J. Yoo, J. B. Park and Y. H. Choi, "Stable predictive control of chaotic systems using self-recurrent wavelet neural network," *Int. J. Control Autom. Syst.* **3**(1), 43–55 (2005).
37. V. Santibañez, K. Camarillo, J. Moreno-Valenzuela and R. Campa, "A practical PID regulator with bounded torques for robot manipulators," *Int. J. Control Autom. Syst.* **8**(3), 544–555 (2010).
38. J. Huang, C. Wen, W. Wang and Z.-P. Jiang, "Adaptive stabilization and tracking control of a nonholonomic mobile robot with input saturation and disturbance," *Syst. Control Lett.* **62**(3), 234–241 (2013).
39. M. Chen, B. Jiang, J. Zou and X. Feng, "Robust adaptive tracking control of the underwater robot with input nonlinearity using neural networks," *Int. J. Comput. Intell. Syst.* **3**(5), 646—655 (2010).
40. Y. Li, S. S. Ge and C. Yang, "Learning impedance control for physical robot–environment interaction," *Int. J. Control* **85**(2), 182–193 (2012).

Mohammad Hossein Hamedani was born in Tehran, Iran. He received the B.Sc. degree in robotics engineering from Shahrood University, Shahrood, Iran, in 2010, and the M.Sc. degree in mechatronics engineering from Khaje Nasir University, Tehran, Iran, in 2013. He is currently working toward the Ph.D. degree in electrical engineering (control) with Isfahan University of Technology, Isfahan, Iran, from 2015. His research interests include control systems design, analysis and implementation of mechatronics systems, robotics kinematics and dynamics, artificial intelligence and soft computing.

Maryam Zekri received the Ph.D. degree in electrical engineering (control) from Isfahan University of Technology, Isfahan, Iran, in 2008. She is currently an Associate Professor with the Department of Electrical and Computer Engineering, Isfahan University of Technology. Her research interests include the area of soft computing (wavelet network, neural network, and fuzzy logic), intelligent control and automatic diagnosis of diseases.

Farid Sheikholeslam received the B.Sc. degree in electronics from Sharif University of Technology, Tehran, Iran, in 1990, the M.Sc. degree in communications, and the Ph.D. degree in electrical engineering from Isfahan University of Technology (IUT), Isfahan, Iran. Since 1999, he has been cooperating with the Department of Electrical and Computer Engineering, IUT. His research interests include robotics, control algorithms, fuzzy systems, neural networks, stability analysis and nonlinear systems.

https://doi.org/10.1017/S0263574718000930 Published online by Cambridge University Press